Phase Field Modeling of Microstructure

Yunzhi Wang
Department of Materials Science and Engineering
The Ohio State University
Columbus, OH

Aknowledgement
D3D team members
Prof. M.J. Mills; Prof. R. Duherty; Dr. D. Dimiduk
Dr. N. Ma, C. Shen; M. Grober

Input/Output for Phase Field Modeling of Microstructure

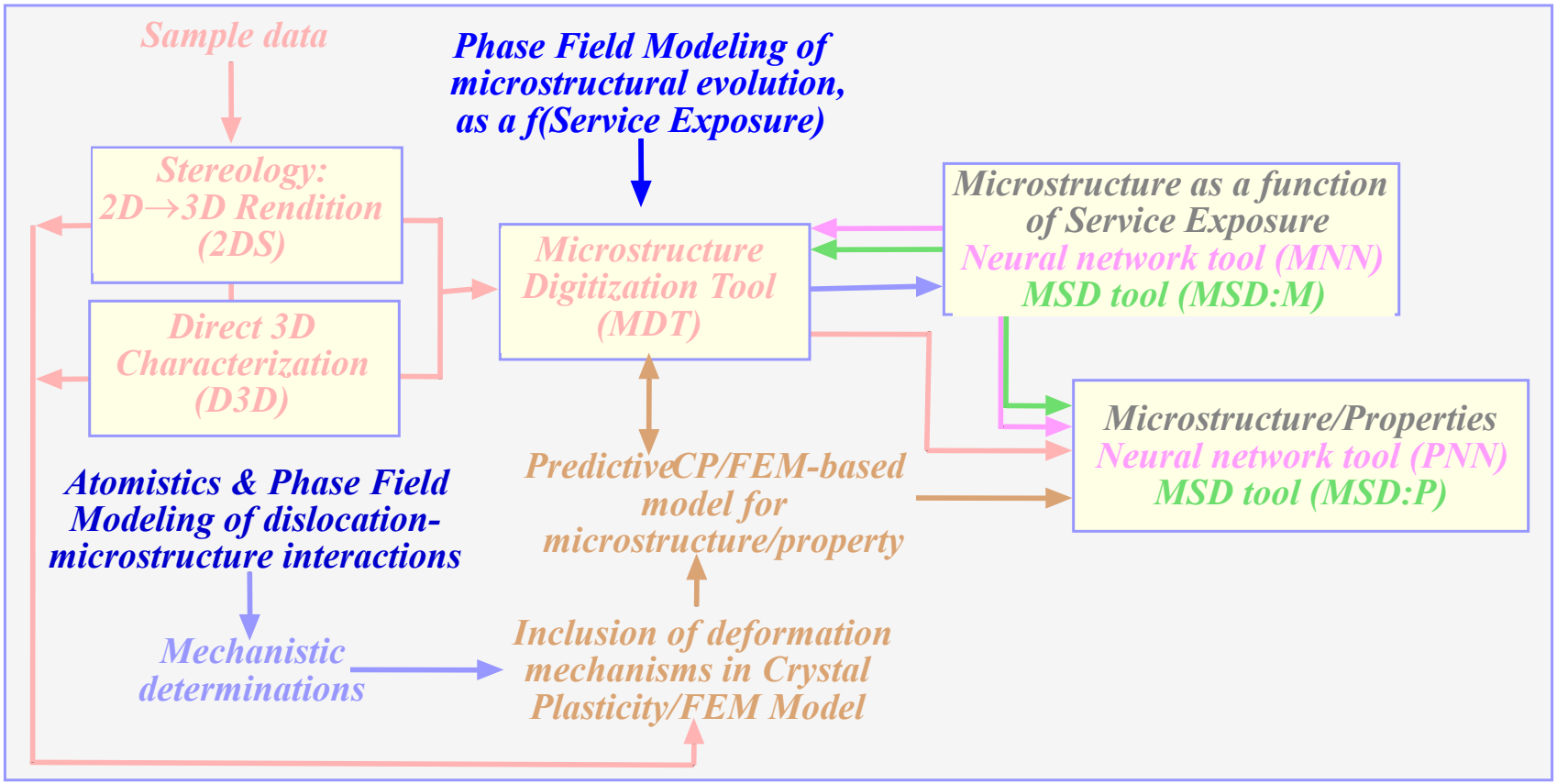

Colony Microstructures in α/β Titanium Alloys

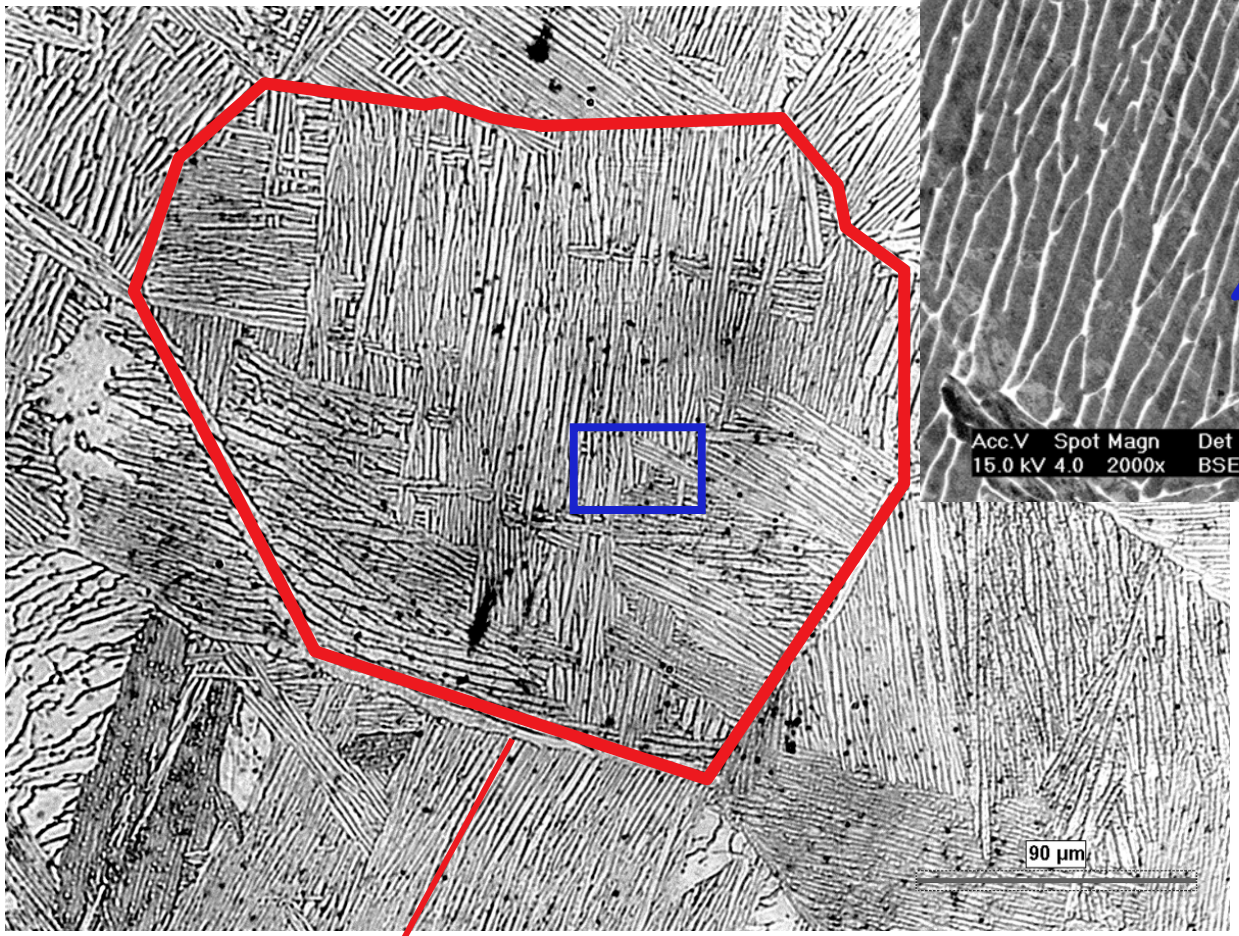

"Prior β" Grain Boundaries

Colony Boundaries

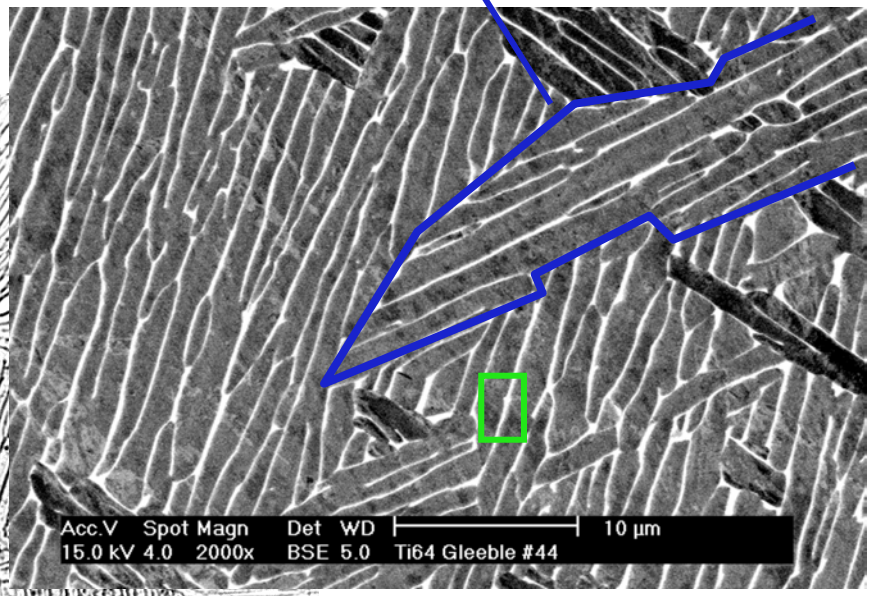

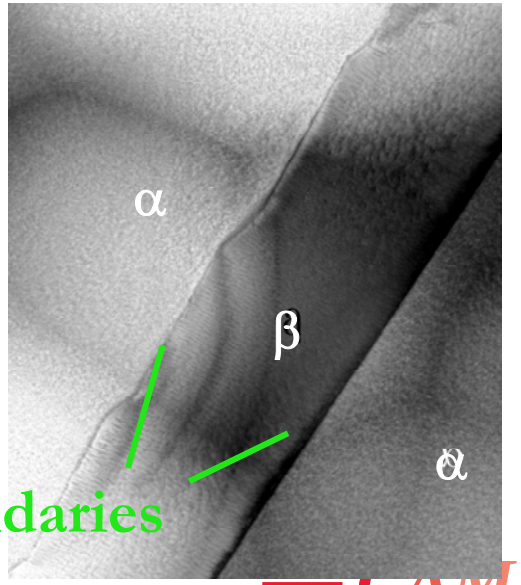

α/β Lath Boundaries

M.J. Mills (OSU)

Orientation relationship and slip vector mismatch

$(101)_\beta \parallel (0001)_\alpha, [1\bar{1}\,\bar{1}]_\beta \parallel [2\bar{1}\,\bar{1}0]_\alpha$

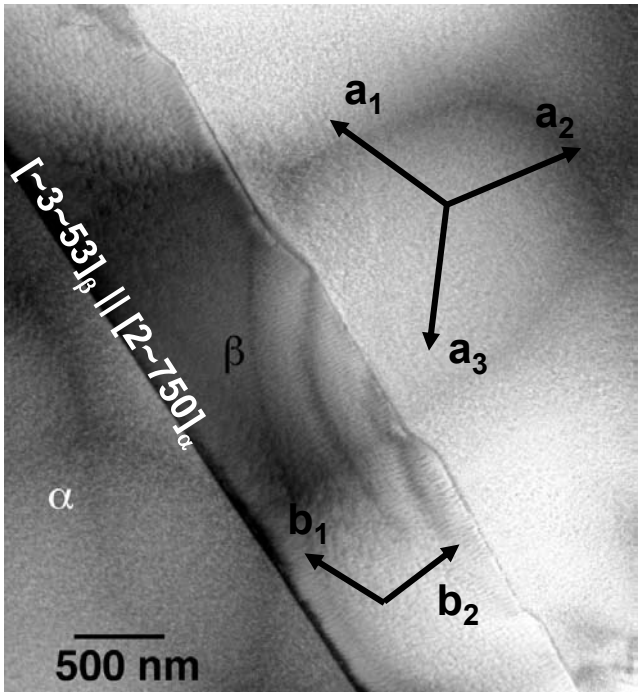

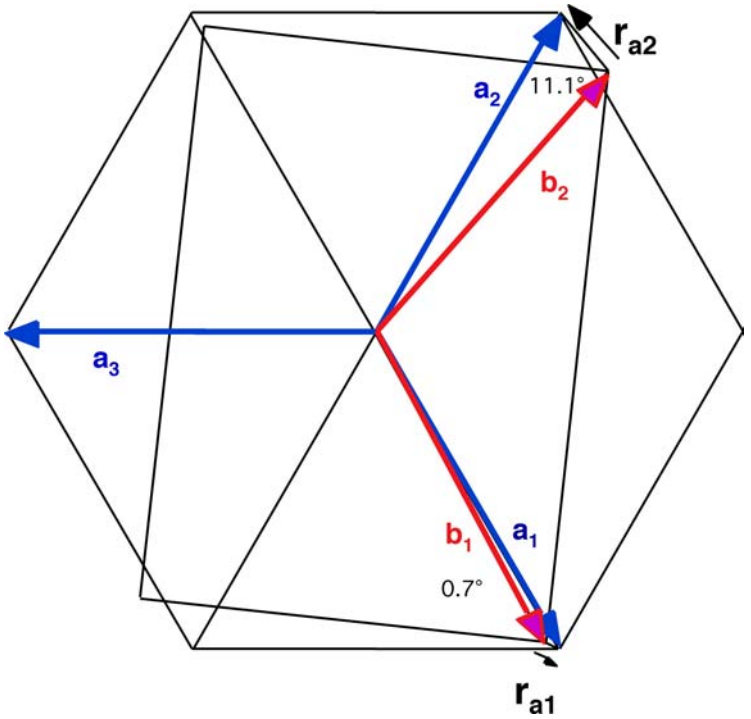

- *Effectively creates three unique slip directions in the α/β colony*

- a_1 and b_1 misoriented by 0.56°
- a_2 and b_2 misoriented by 11.5°
- a_3 has no mating slip vector in β-phase

Anisotropy of α/β Colonies in Compression

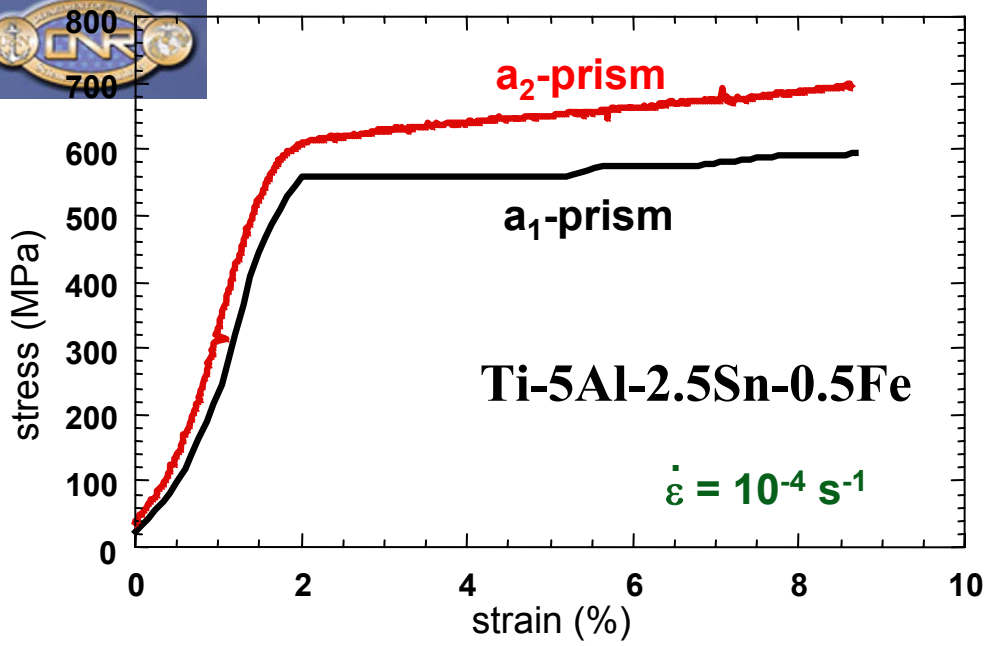

Significant differences in yield and hardening

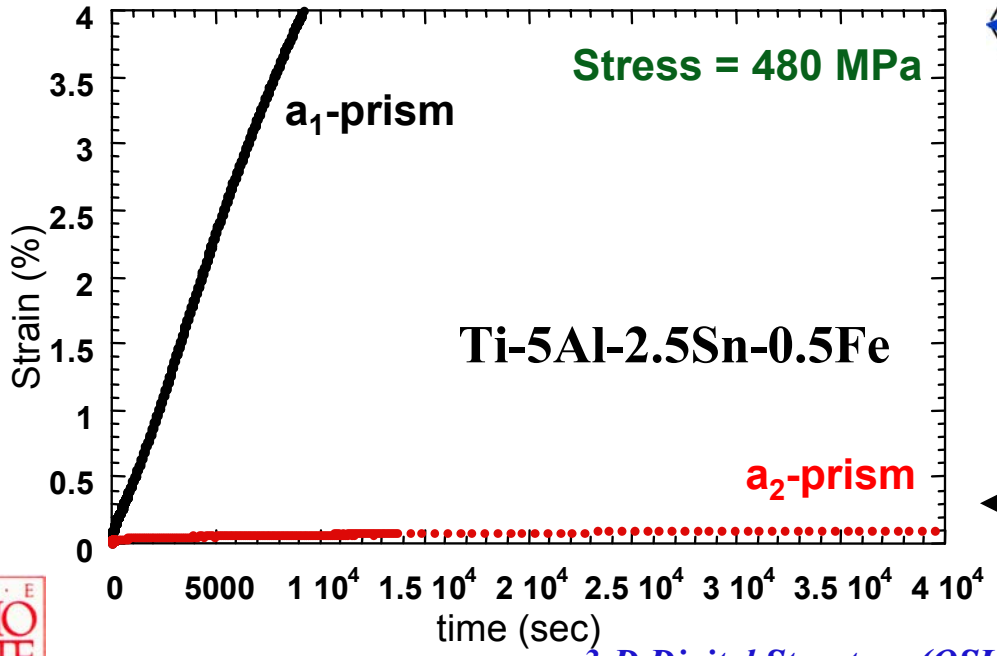

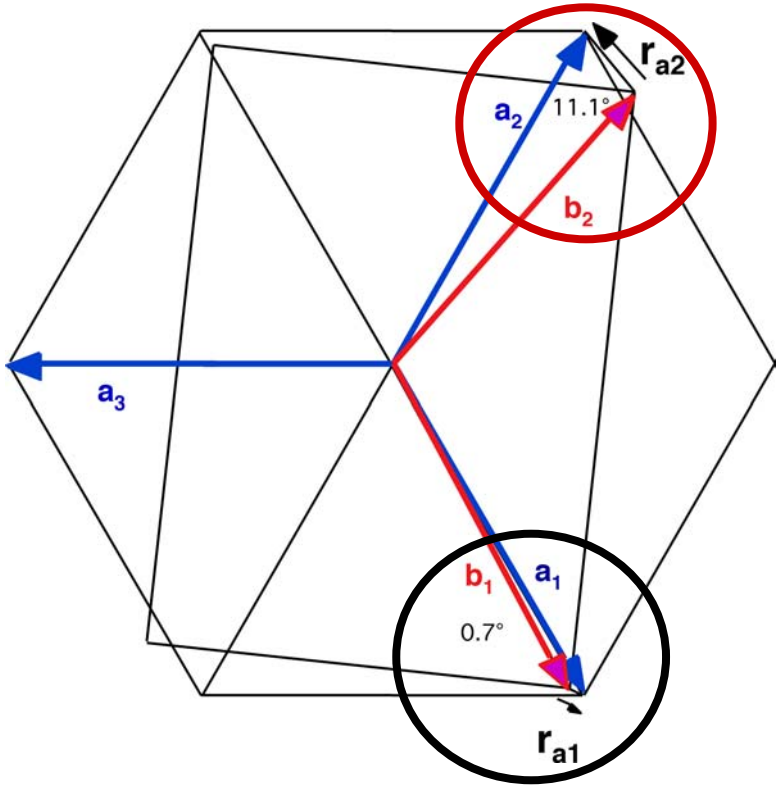

Remarkable differences in creep response

Dislocation-precipitate interactions

- Residual matrix dislocations of a_1 (at entrance interface) and a_3 (at exit interface)

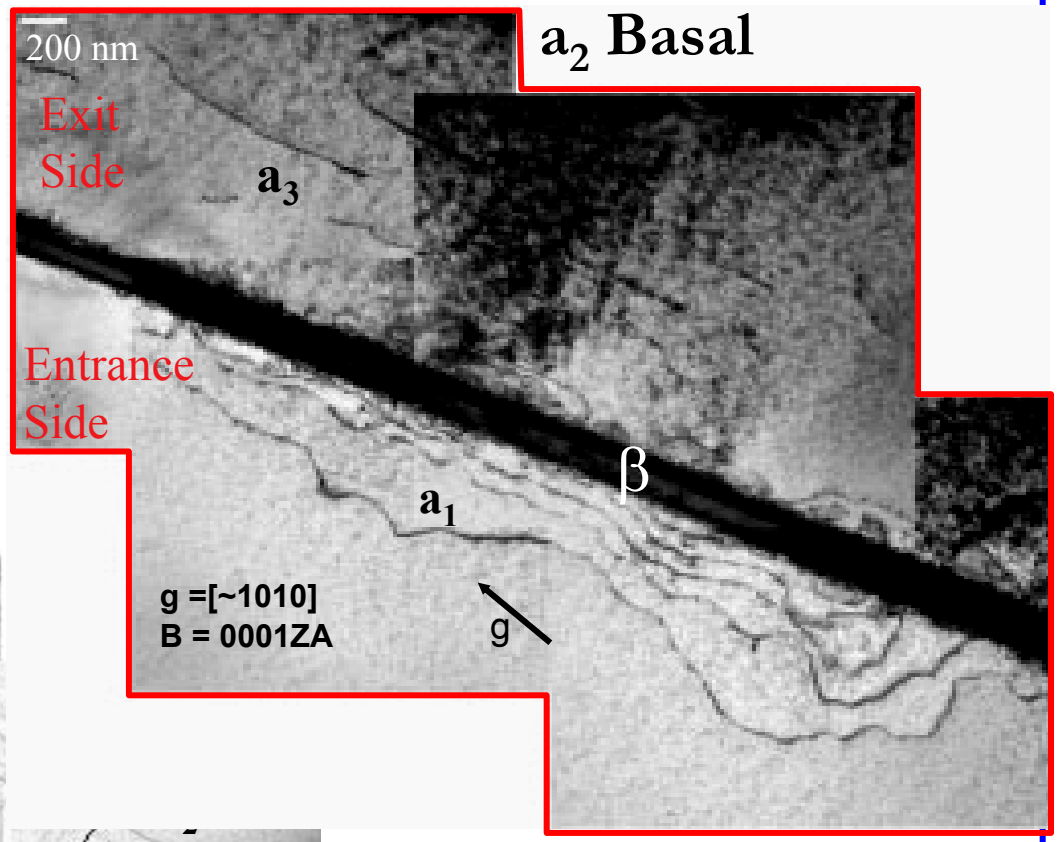

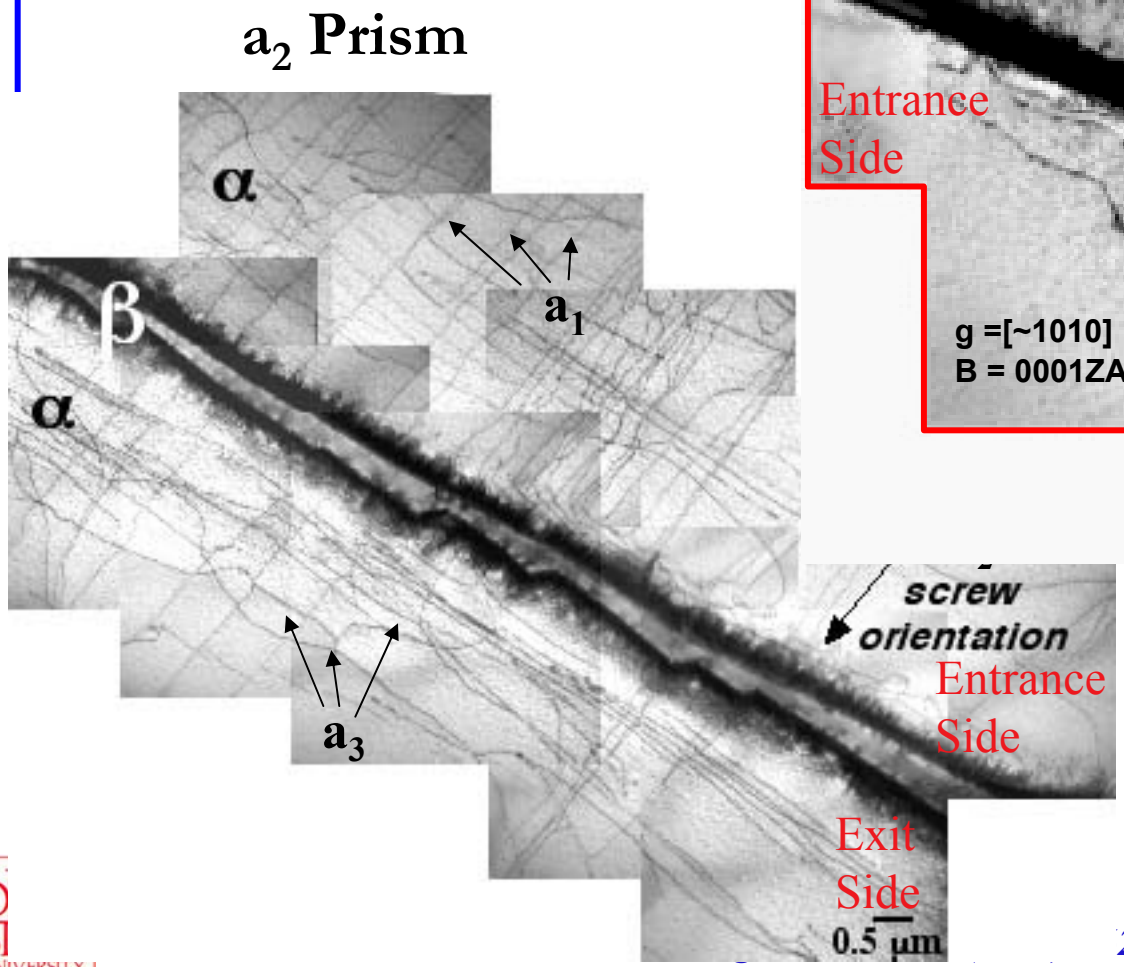

- Present *only* near regions undergoing slip transmission

Ti 550 - Slip Accumulation Studies

Total plastic strain 1 %

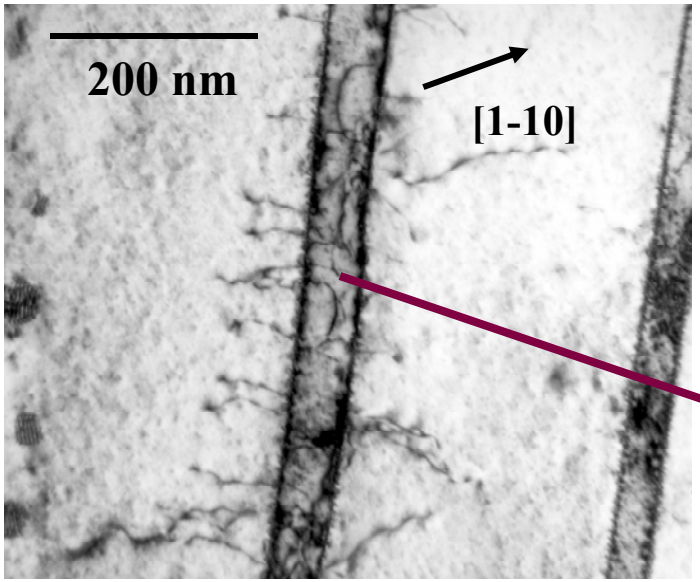

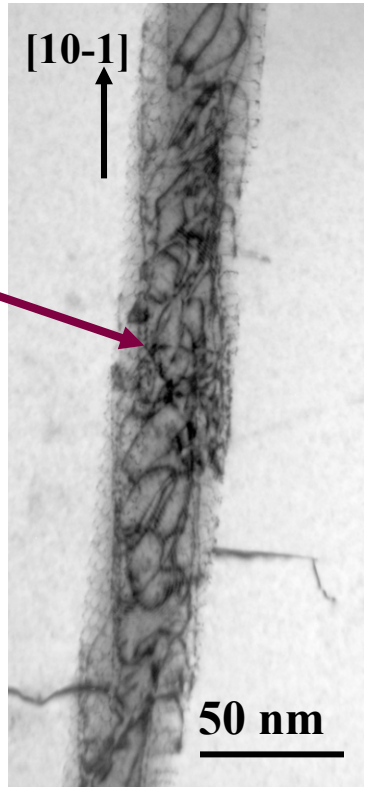

Total plastic strain 5 %

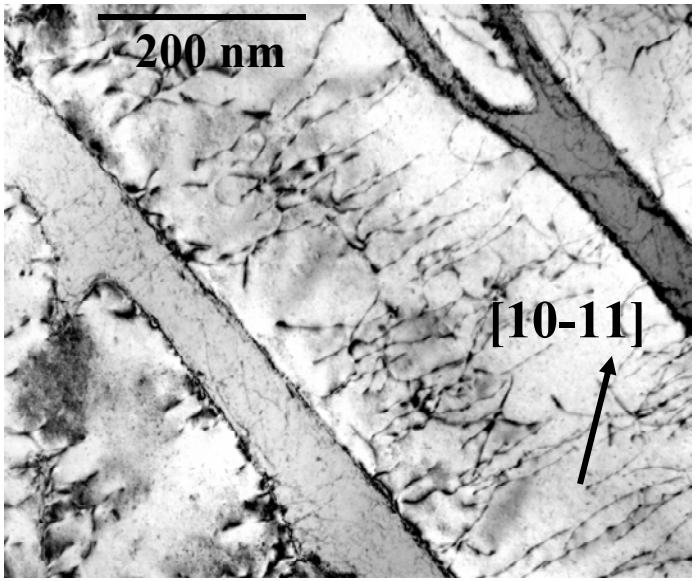

B. Viswanathan and H.L. Fraser

γ/γ′ Microstructure in Ni-Base Superalloys

Disk alloy: sample was soaked above gamma prime and slowly cooled at a linear rate to below 500°C

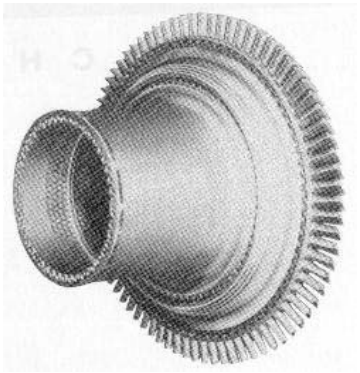

Courtesy of M. F. Henry, GE

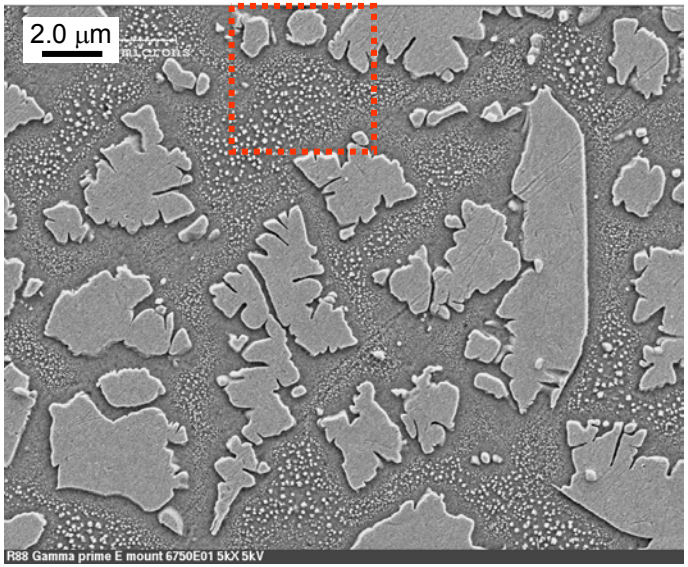

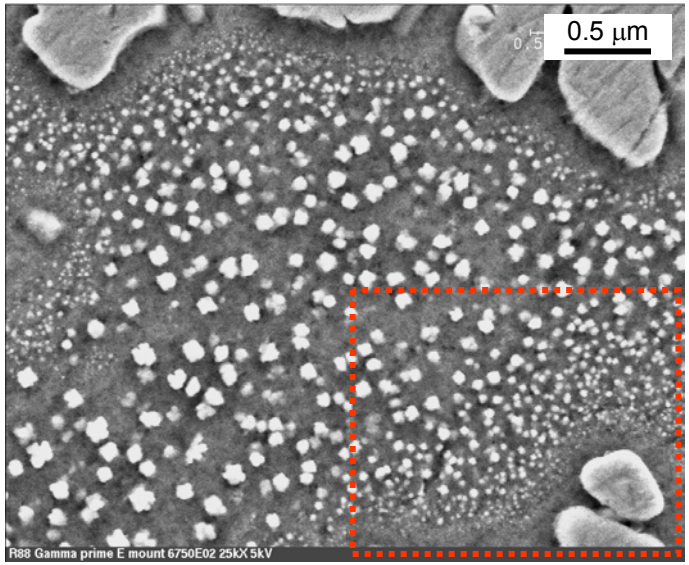

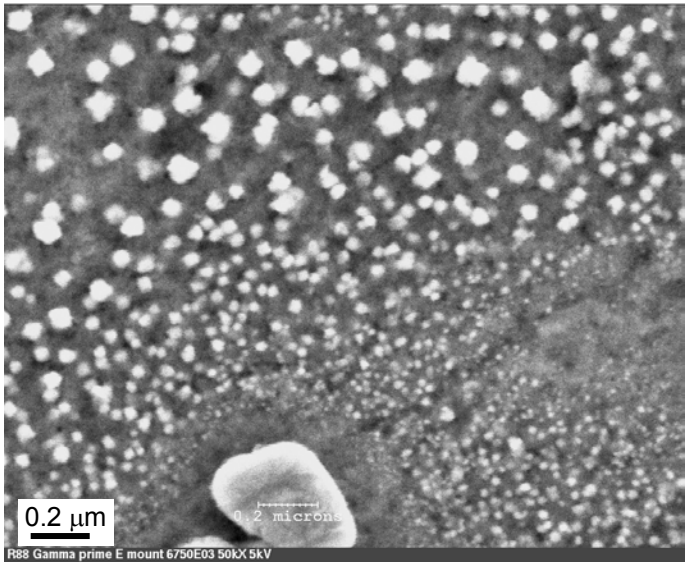

Looping, shearing, and micro-twinning

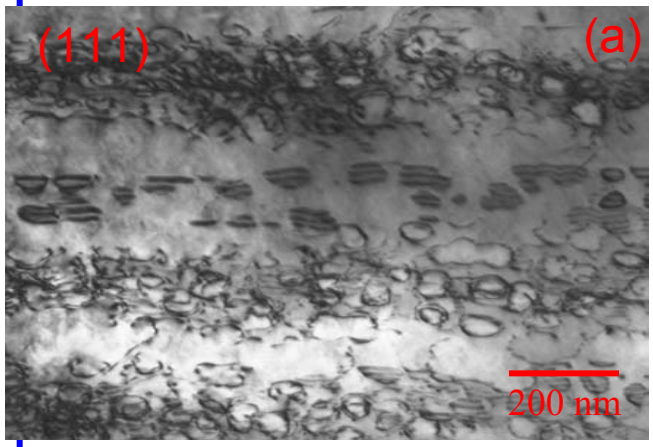

(a) Orowan looping around large precipitates

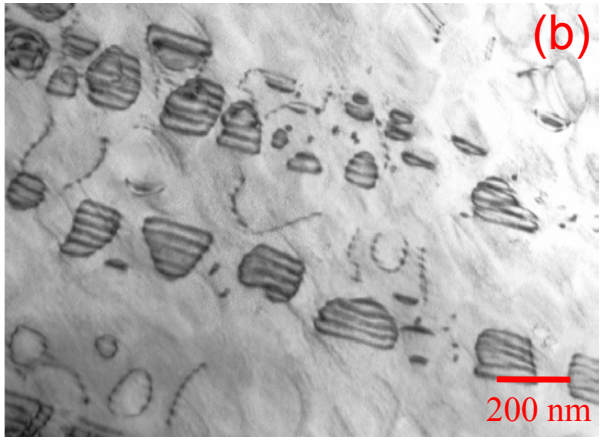

(b) Localized faulting of large precipitates

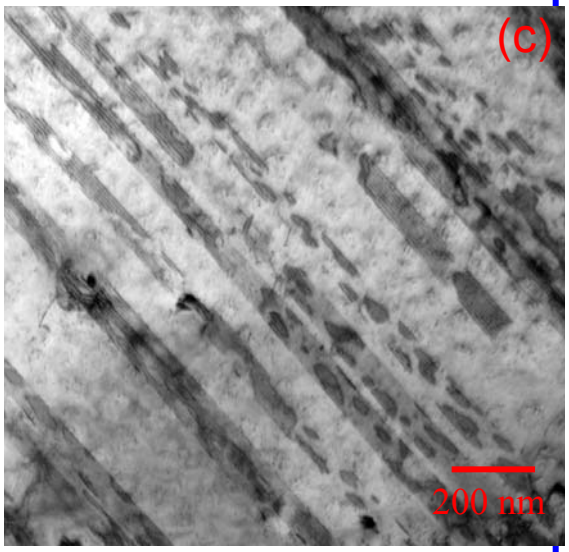

Creep deformation microstructure in Rene 88 after 0.5% Strain under 121 ksi at 650°C
(Courtesy of B. Viswanathan and M. J. Mills)

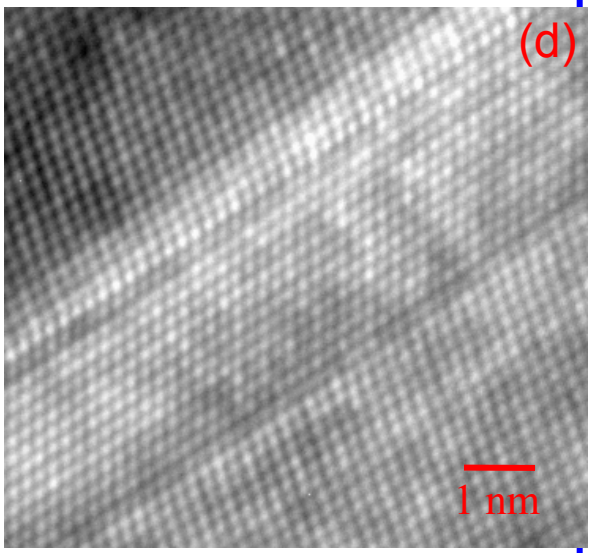

(c) and (d) Continuous faulting (micro-twinning) of both the γ-matrix and γ'-particles

Dramatic Effect of Microstructure Scale On Creep Response

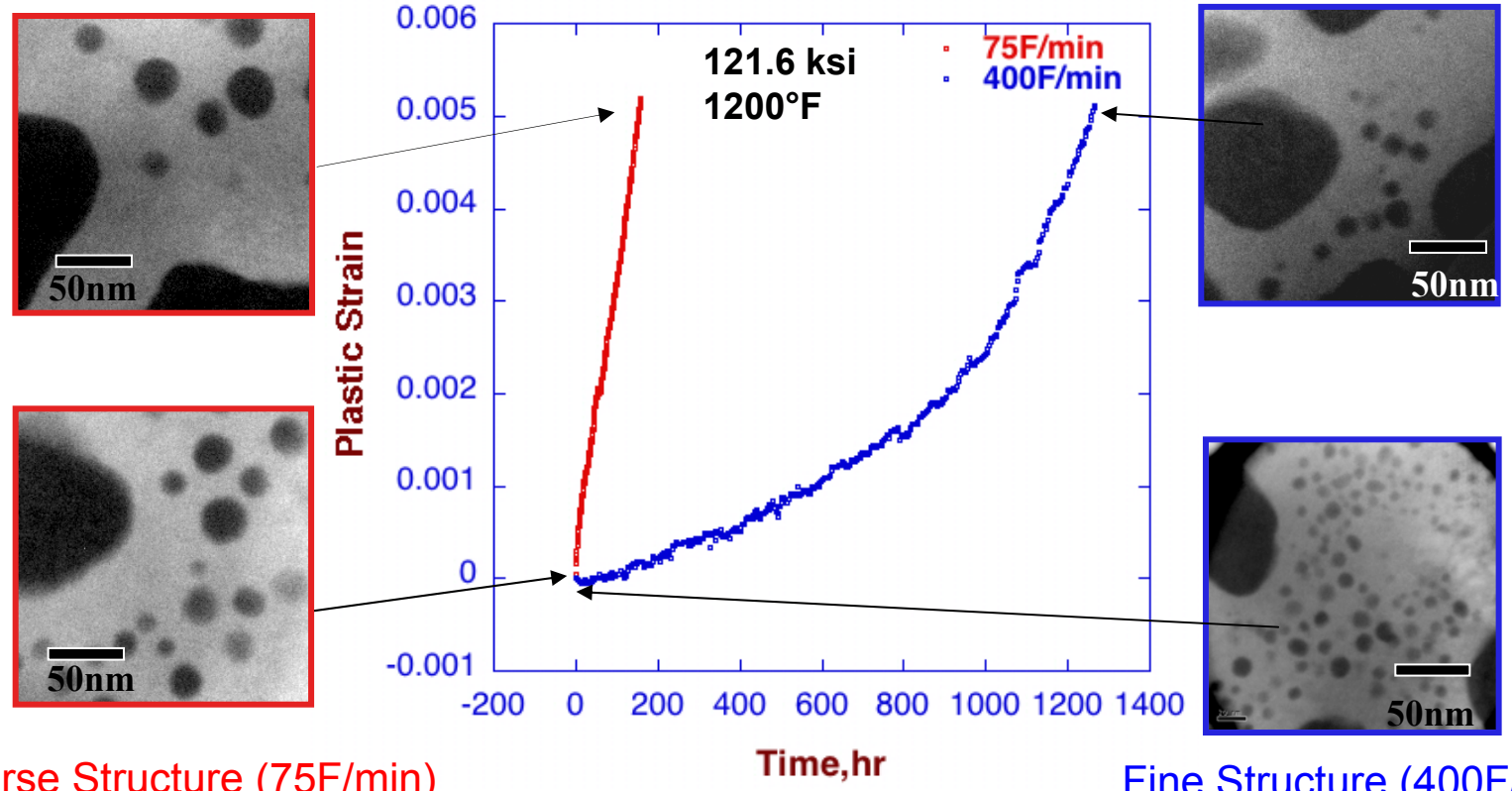

Coarse Structure (75F/min)

Fine Structure (400F/min)

- Strong effect of tertiary volume fraction on creep strength
- Coarsening/dissolution of tertiary population occurs at these temp.
- *Different mechanisms* active for the two microstructures

Development of microstructure- and micromechanim-based models

- Clearly, without these detailed insights into the operative mechanisms, any modeling attempt to describe micro structural evolution and creep deformation in these alloys will remain phenomenological and of limited predictive power.
- A principle theme of our approach is to develop microstructure- and micromechanims-based models that account for the coupling between precipitate microstructure and dislocation activities.

Multi-scale phase field modeling

- Conventional phase field method at mesoscopic scales for microstructural evolution of precipitate and dislocations
- Digital representation and reconstruction of microstructures using phase field method
- Microscopic phase field modeling of dislocation core structures and dislocation-precipitate interactions

Phase Field Modeling of Formation and Coarsening of γ/γ′ Bimodal Microstructures in Ni-Al

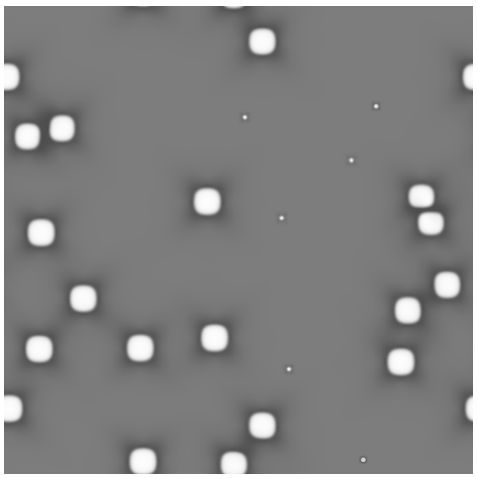

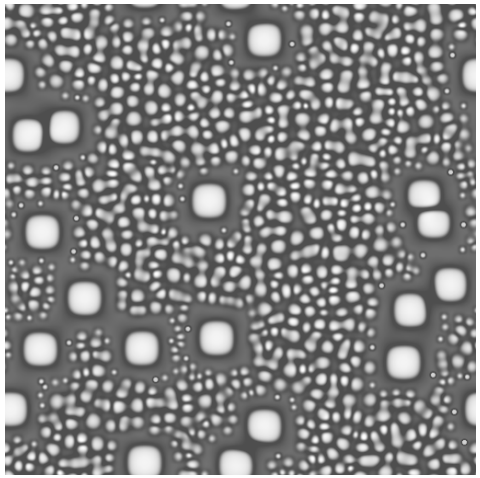

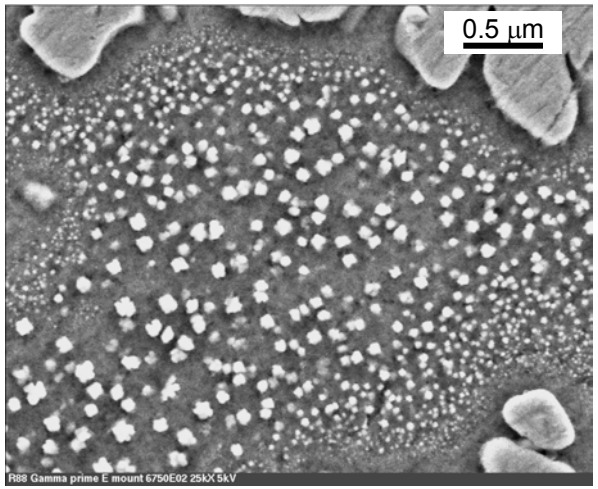

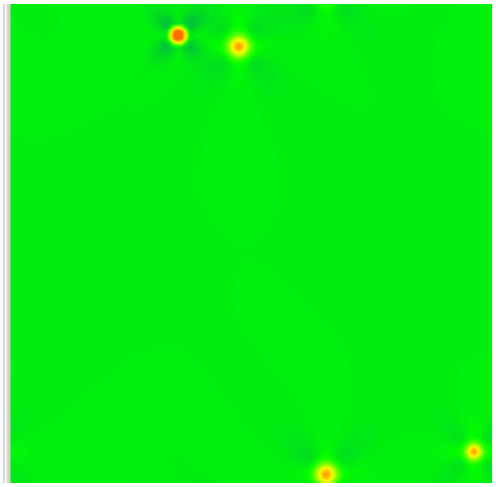

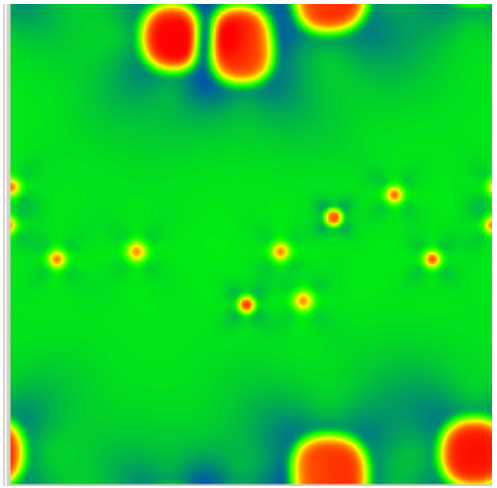

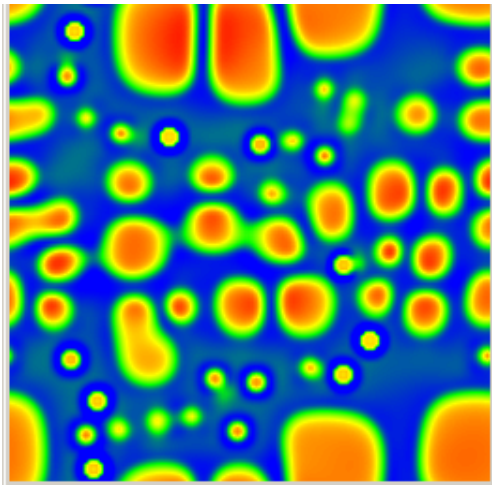

$$\frac{\Delta G^*_{het}}{\Delta G^*_{hom}} = 0.75$$

Continuous cooling + heterogeneous and homogeneous nucleation

- Landau polynomial/sublattice model for free energy
- Diffusivity, interfacial energy, elastic constants and lattice parameter from Ardell's

Update from Billie

3D quantitative phase field model calibration

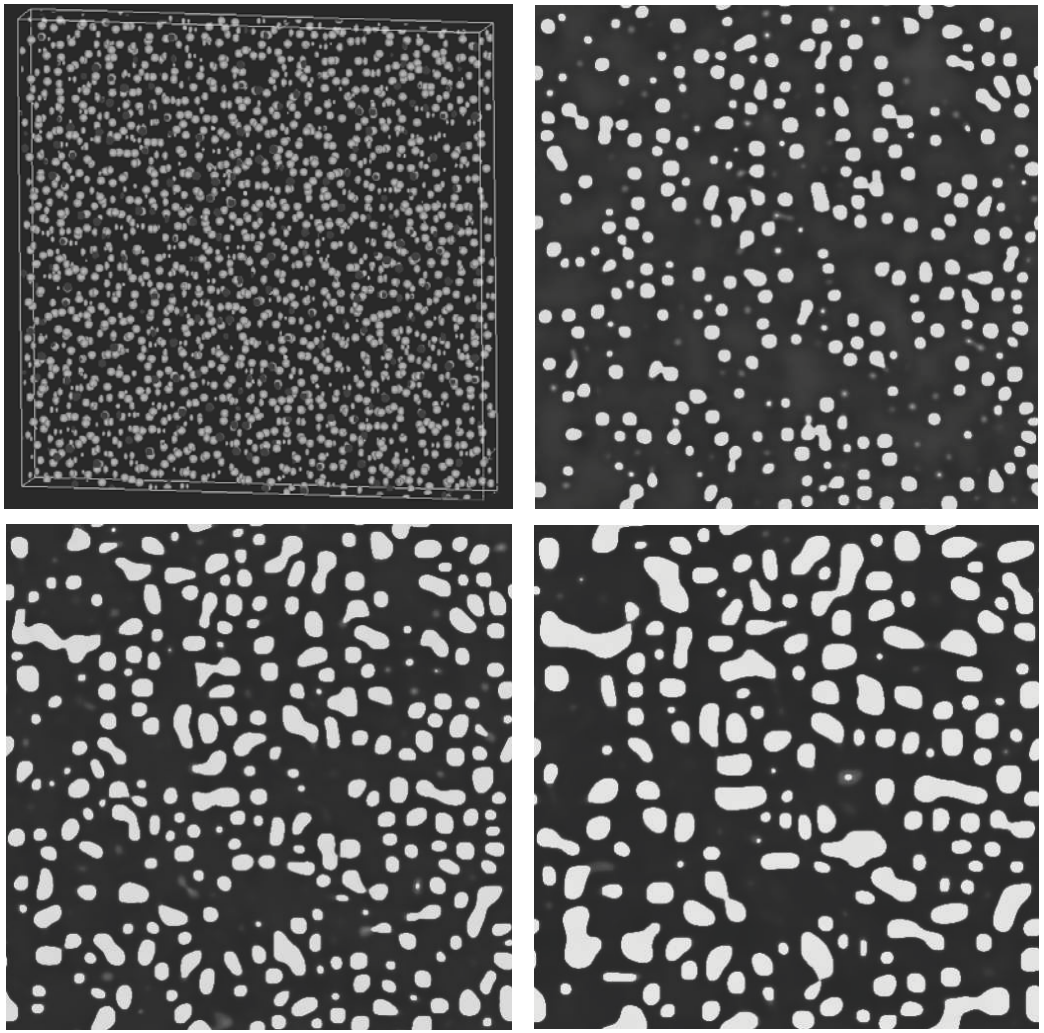

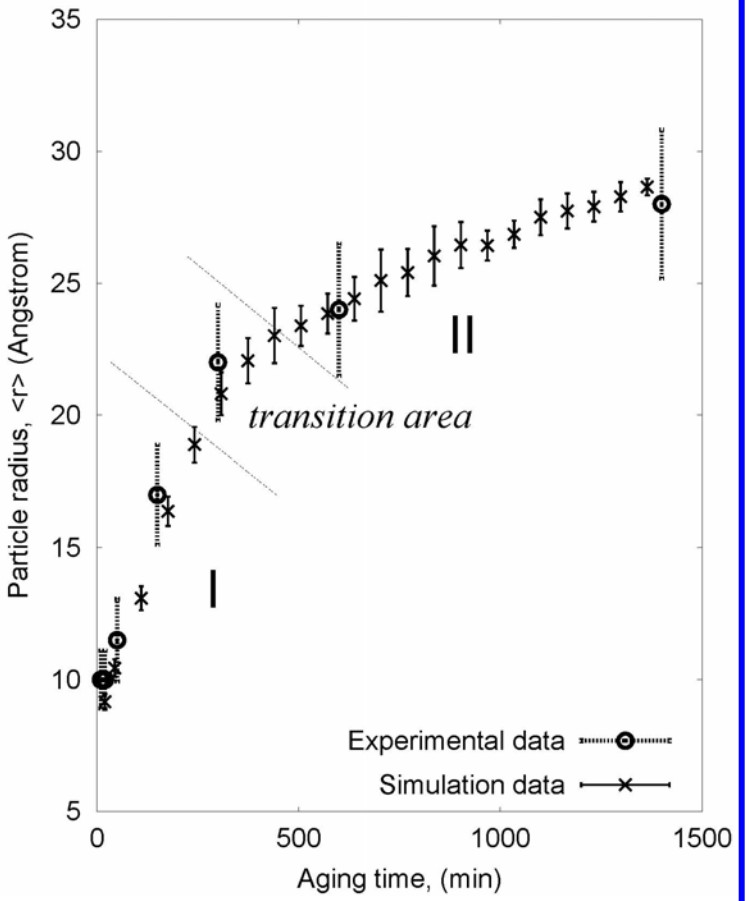

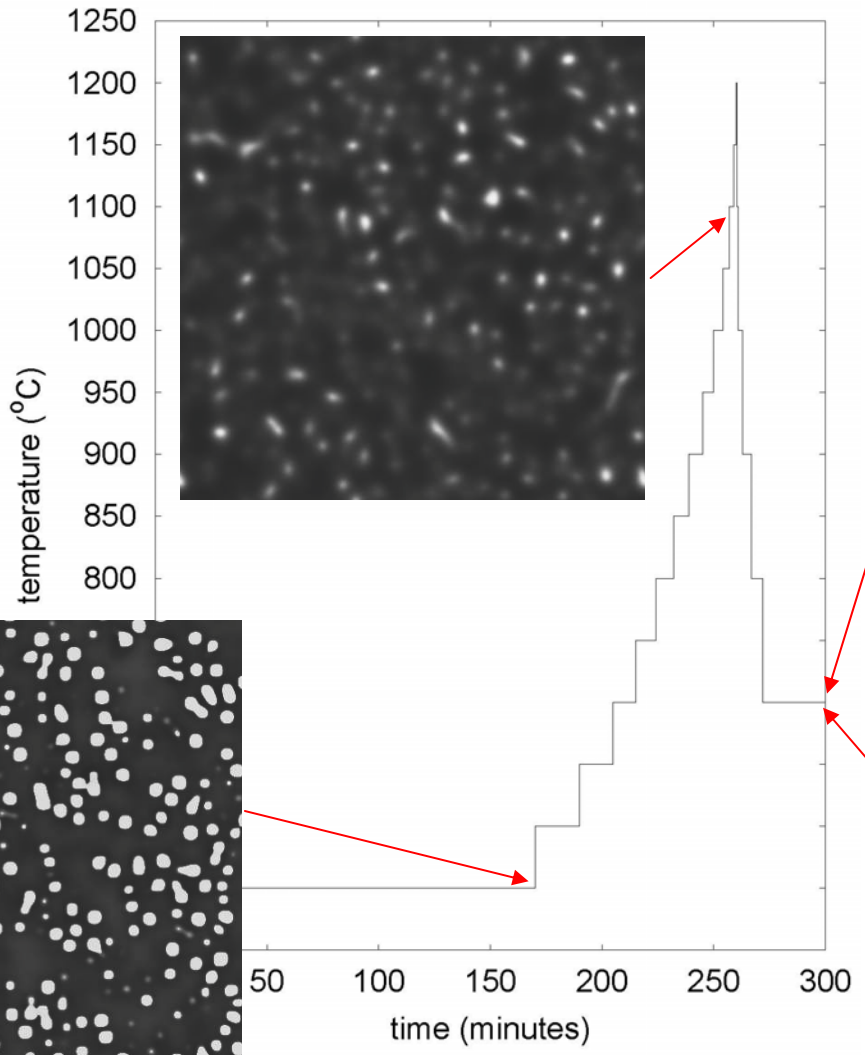

- Input: an arbitrary heat treatment schedule
- Output: digital microstructural evolution
- Model and data are being evaluated by NN, MDT, and MSD

Sensitivity study of various input parameters

Phsse Field Modeling of Microstructure Evolution in Ti-6Al-4V

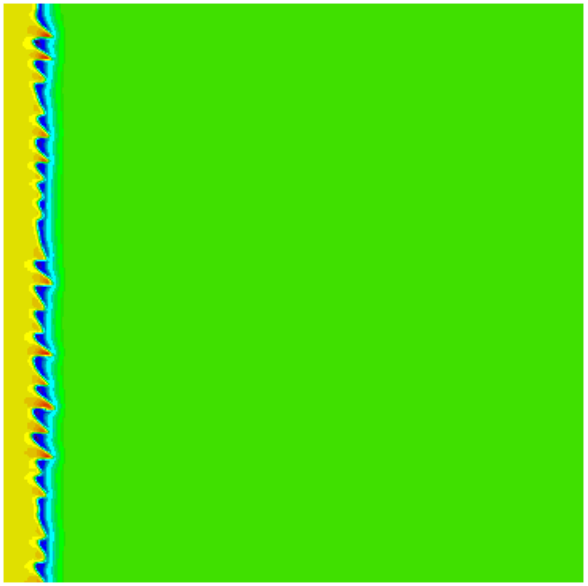

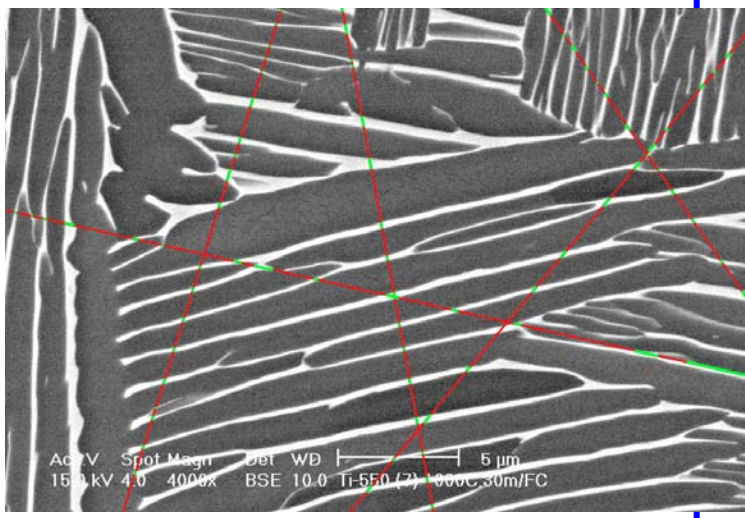

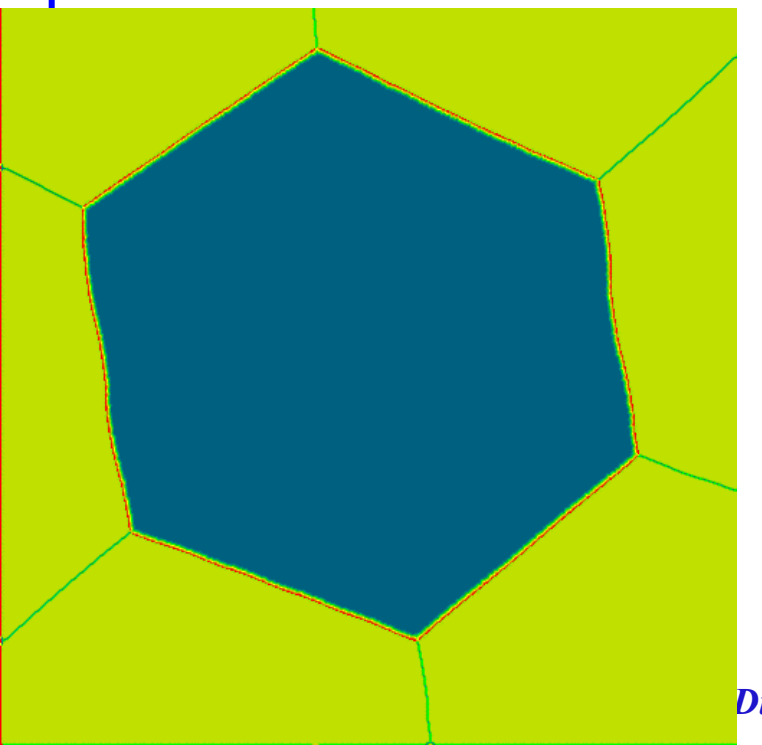

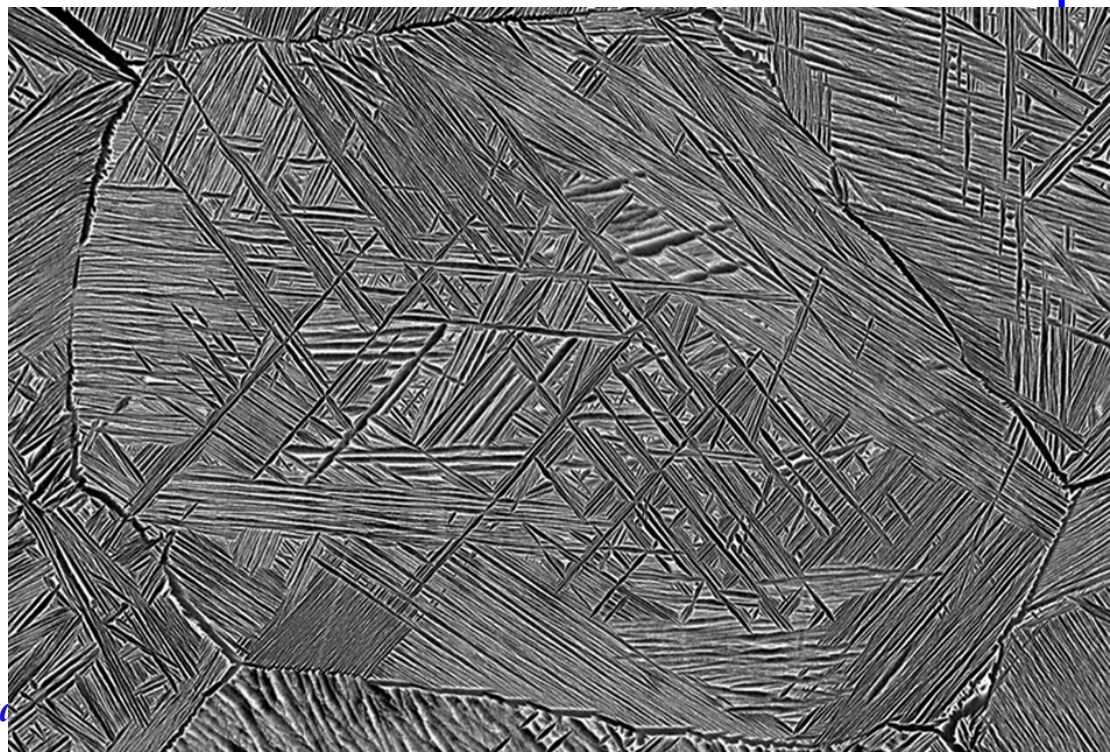

Growth of Globular α – Effect of Spatial and Size Distribution

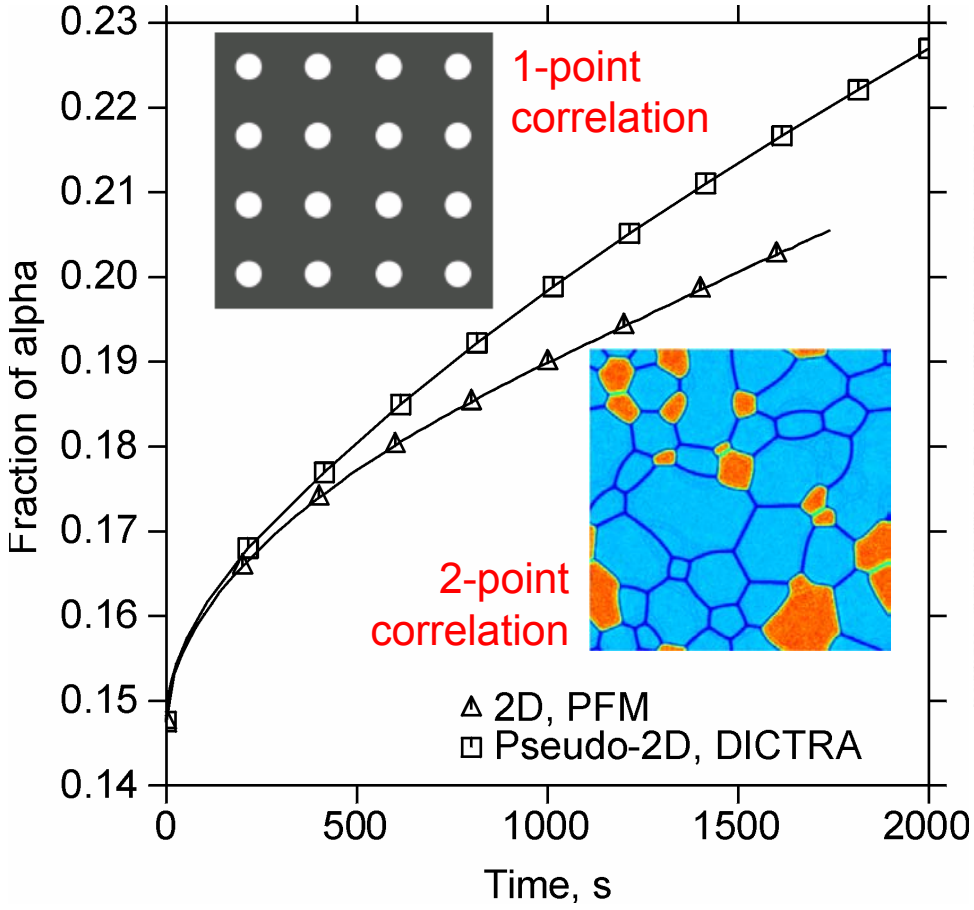

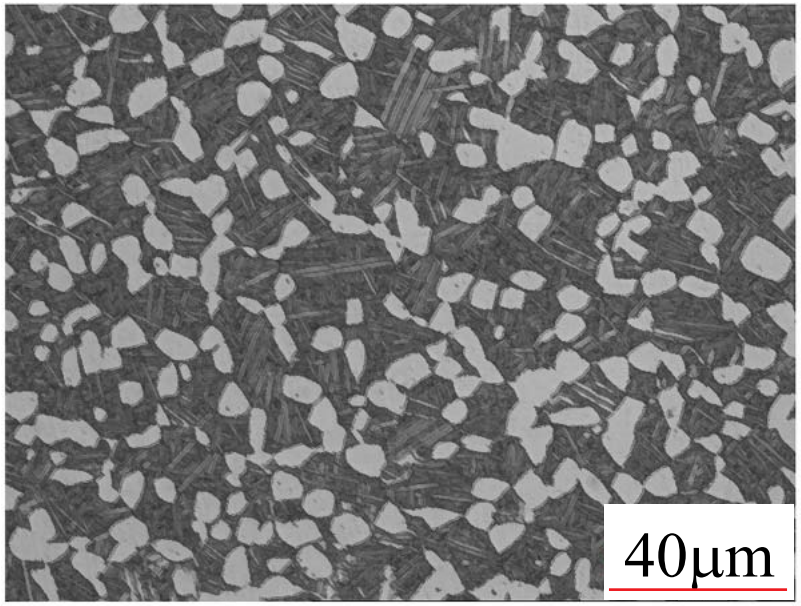

Incorporation of effect from size and spatial distribution

$$f = 1 - \exp\left(-\frac{1}{\xi} \frac{D}{R_f^2} \frac{c_0 - c_\beta}{c_\alpha - c_\beta} t \right)$$

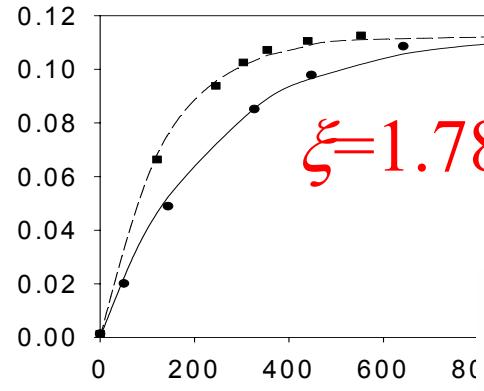

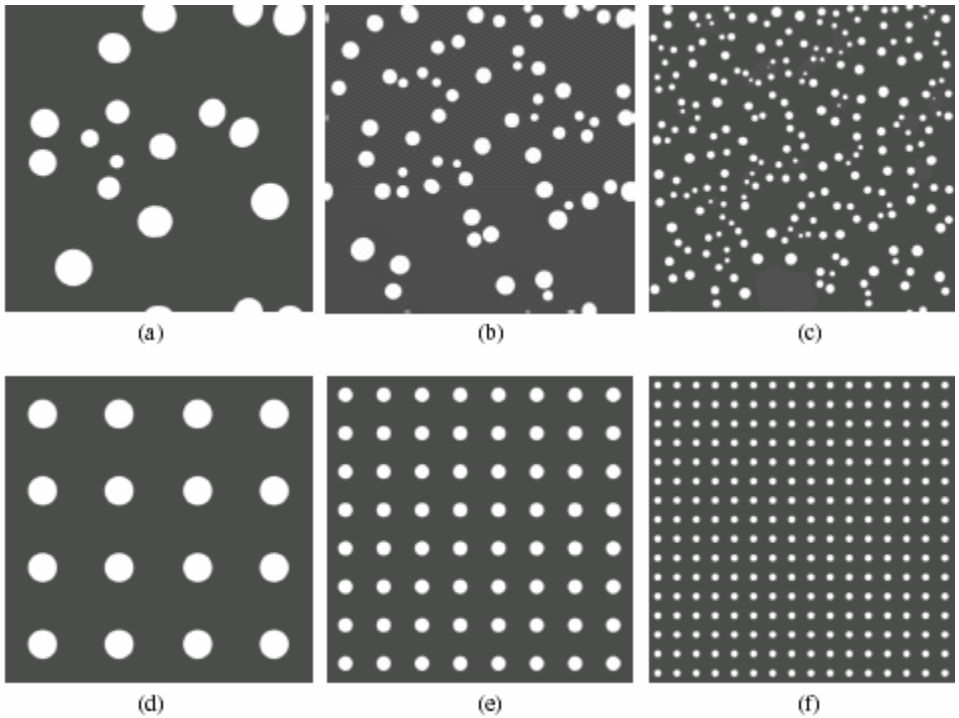

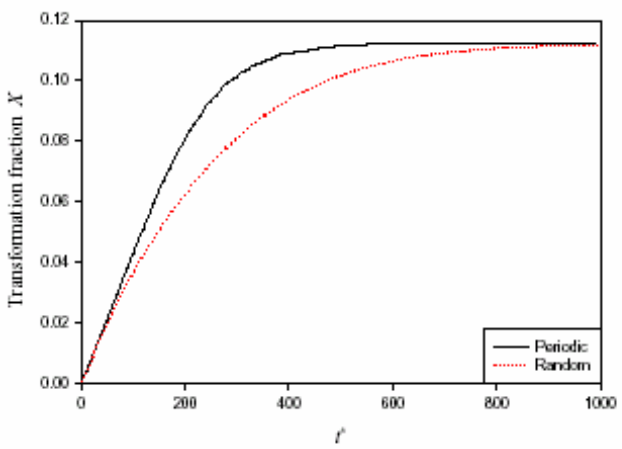

(a)

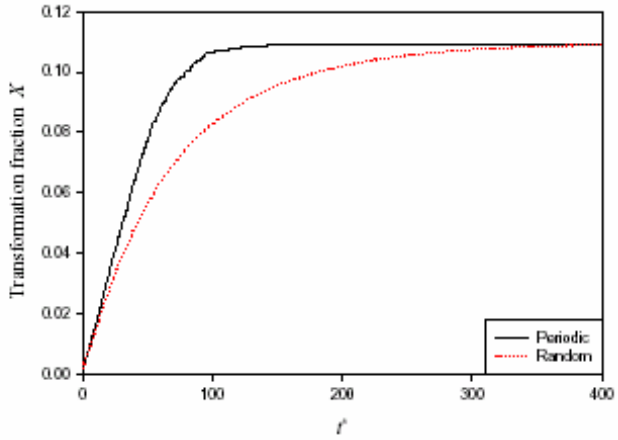

(b)

Mechanisms of recrystallization

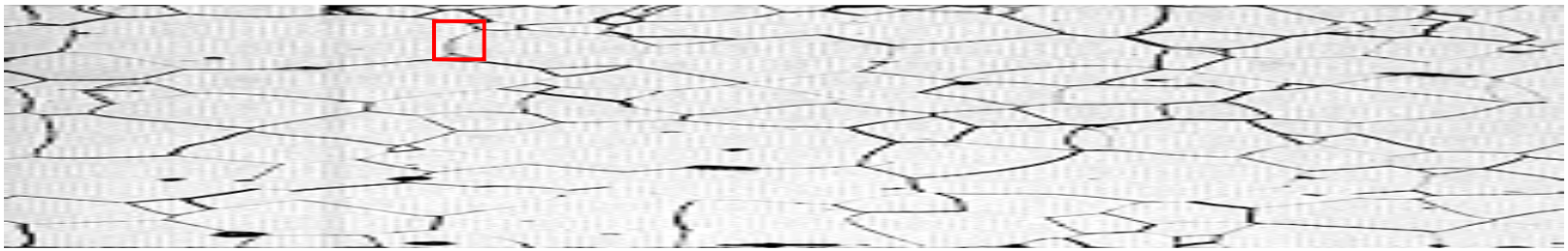

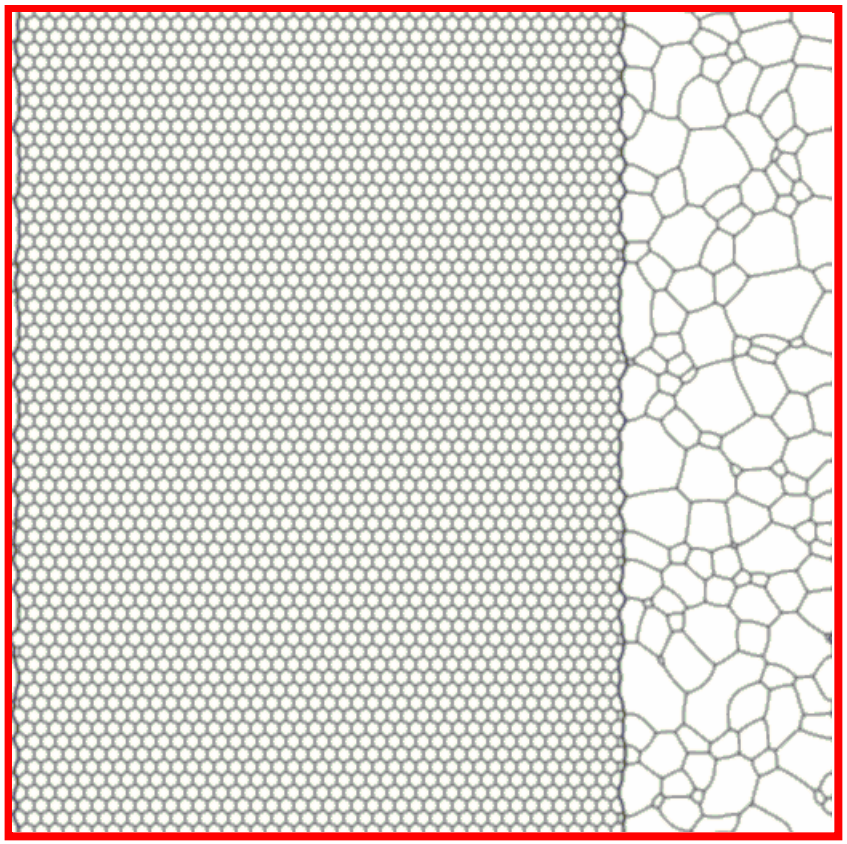

OIM of substructures are being conducted at Drexel

Phase field modeling capability has been developed at OSU

Phase field modeling using OIM as direct input

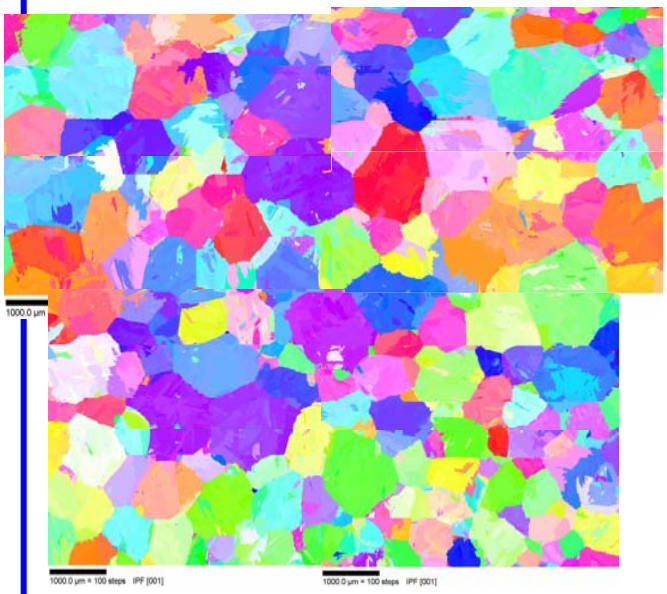

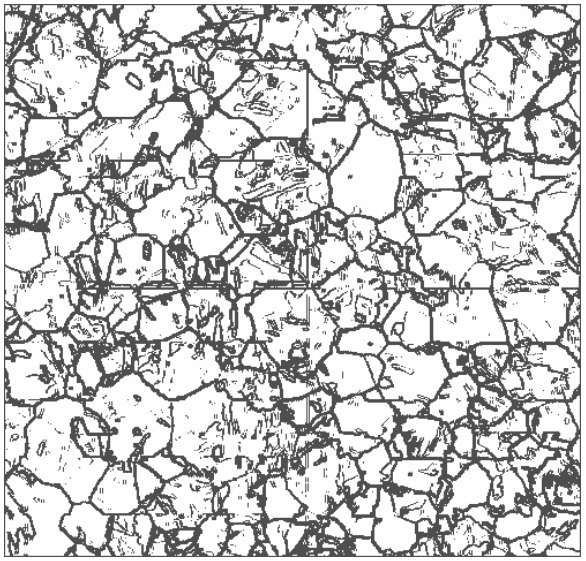

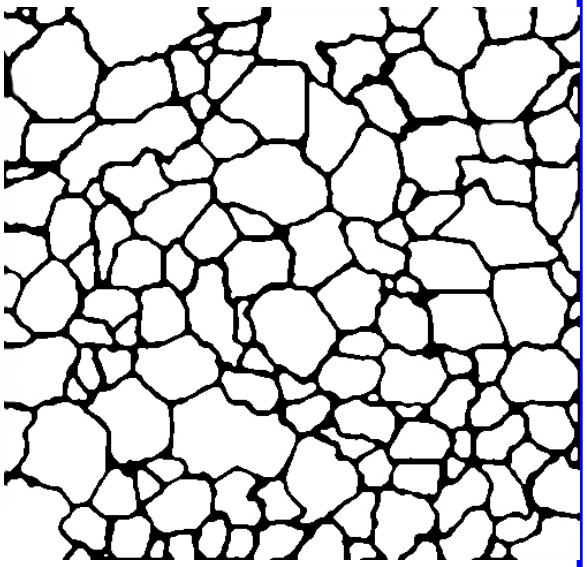

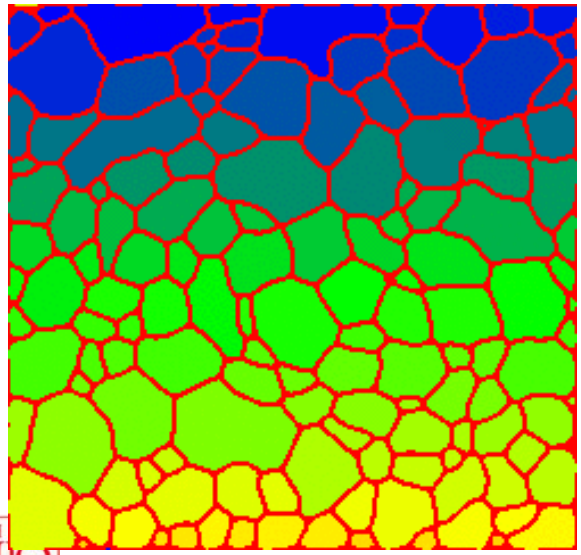

- A software package has been developed to convert automatically OIM data to phase field input

OIM data from Michael G. Glavicic from UES

Sensitivity Study

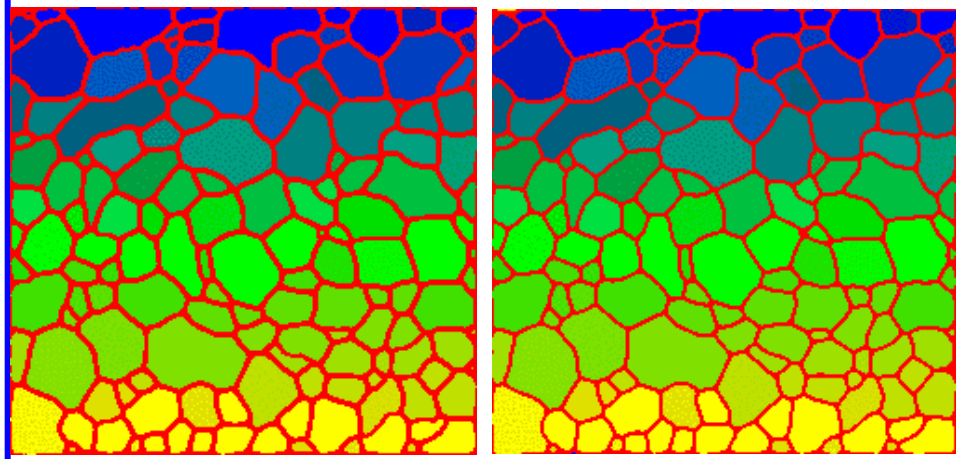

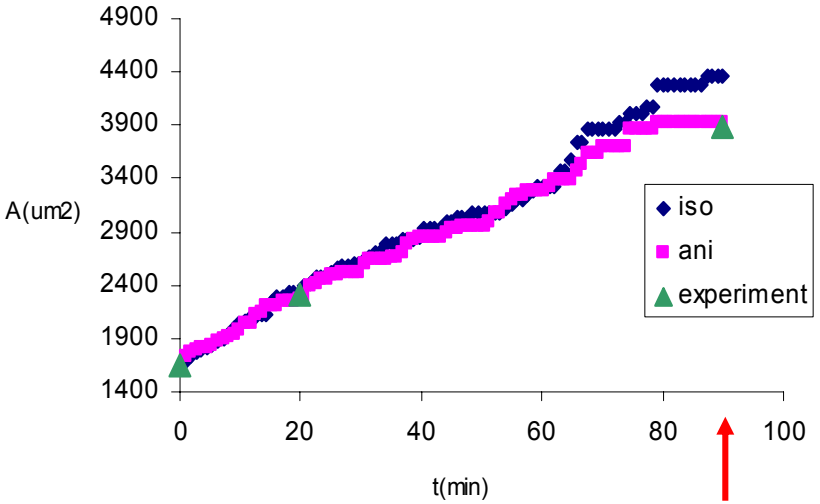

10% difference

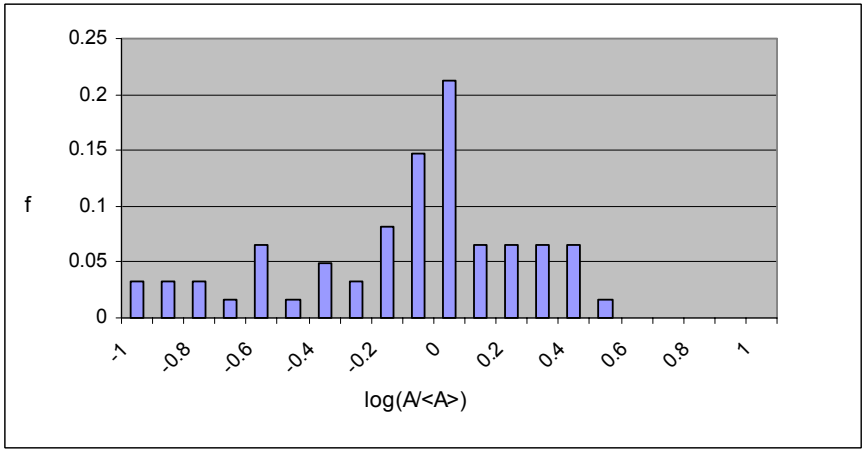

With Texture

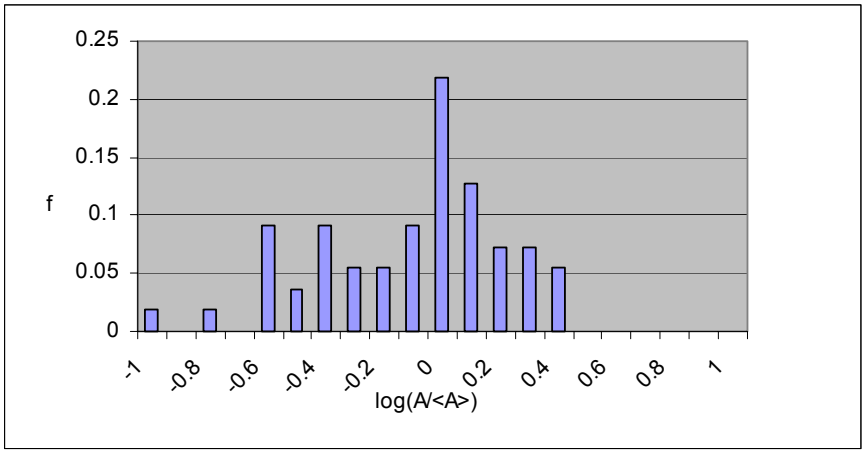

Without Texture

Microstructure reconstruction using phase field

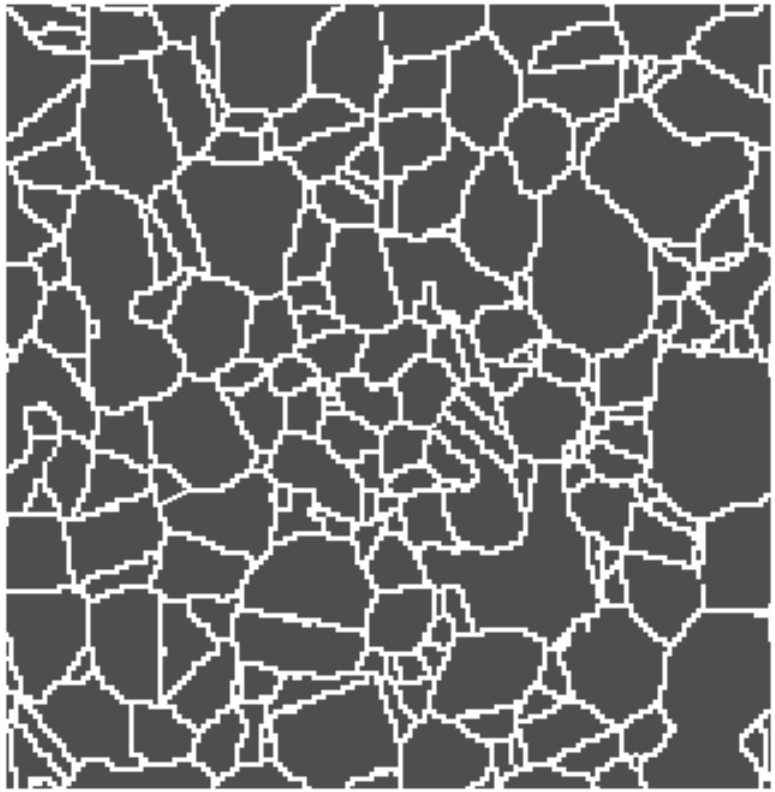

Direct OIM image from Grobhor and Ghosh

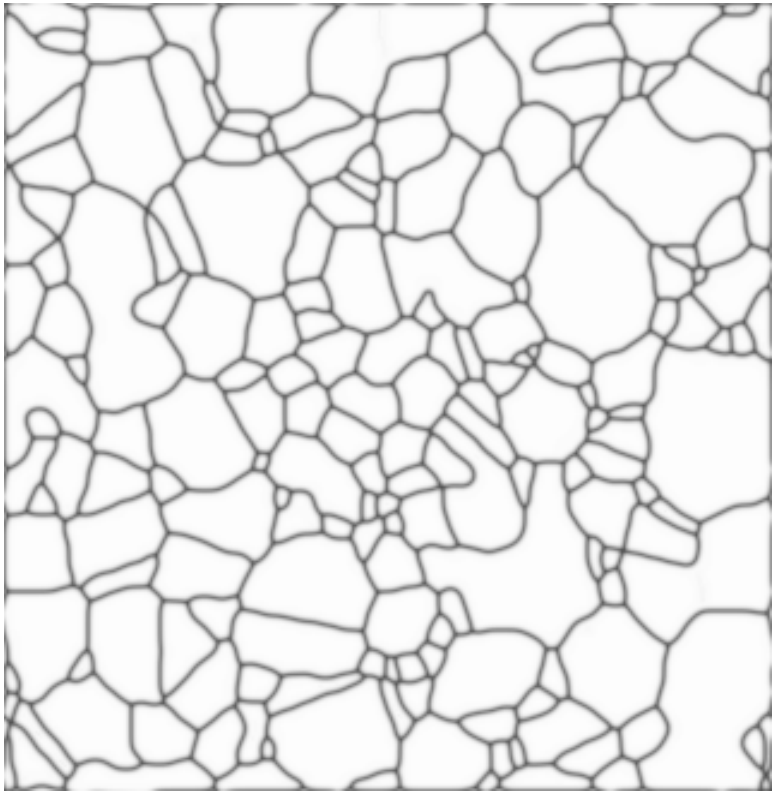

Phase Field Smoothing

Phase field reconstruction using microstructural descriptors (MDF, ODF, micro-texture, size distribution, number of sides, …)– work in progress

Effect of precipitate: Coherent vs Incoherent Interfaces

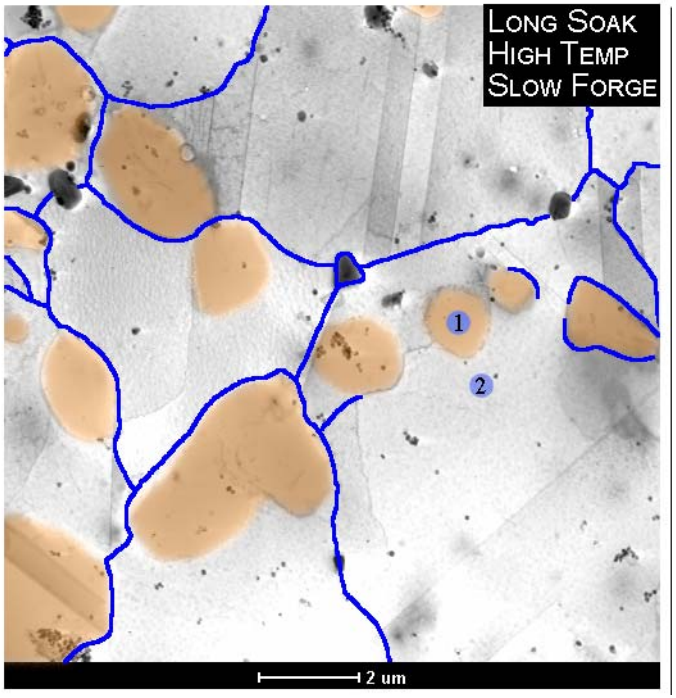

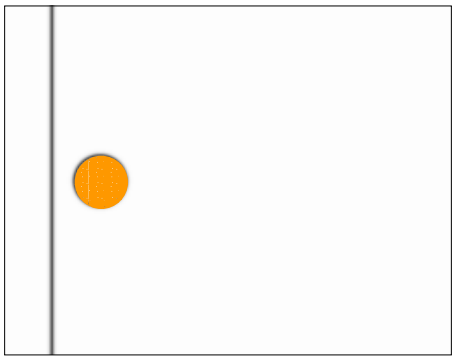

incoherent interfaces

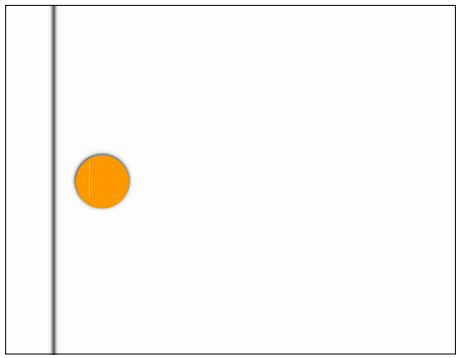

from incoherent to coherent

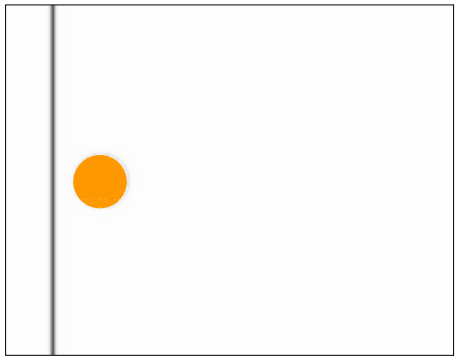

from coherent to incoherent

Orange: Primary gamma prime

Blue: High energy (incoherent) interfaces

Effect of precipitates

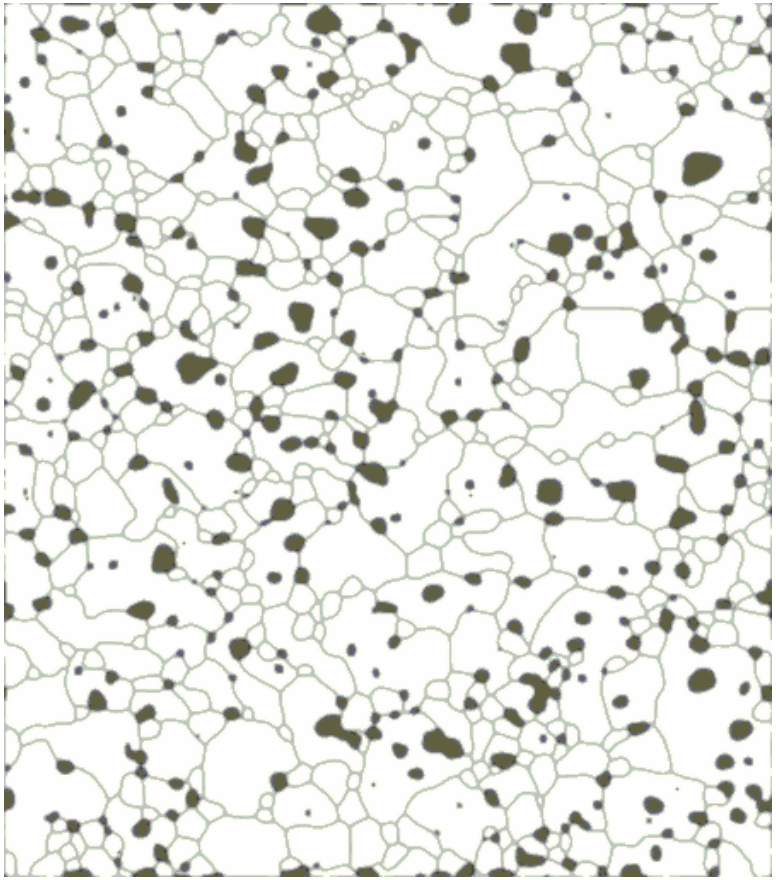

Incoherent

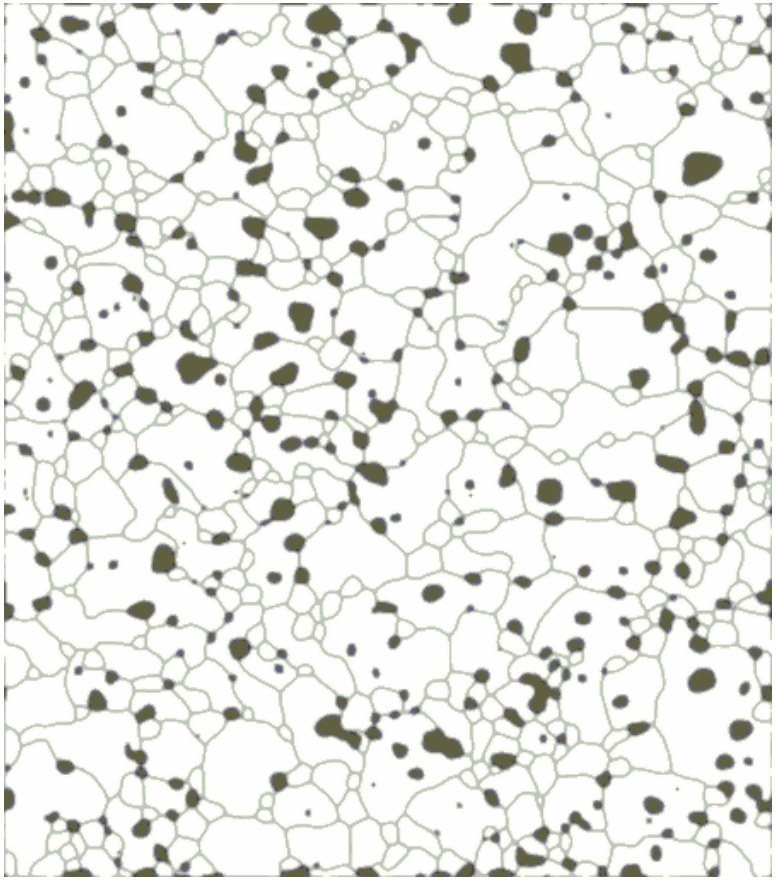

Mixed

Coherent vs incoherent interfaces

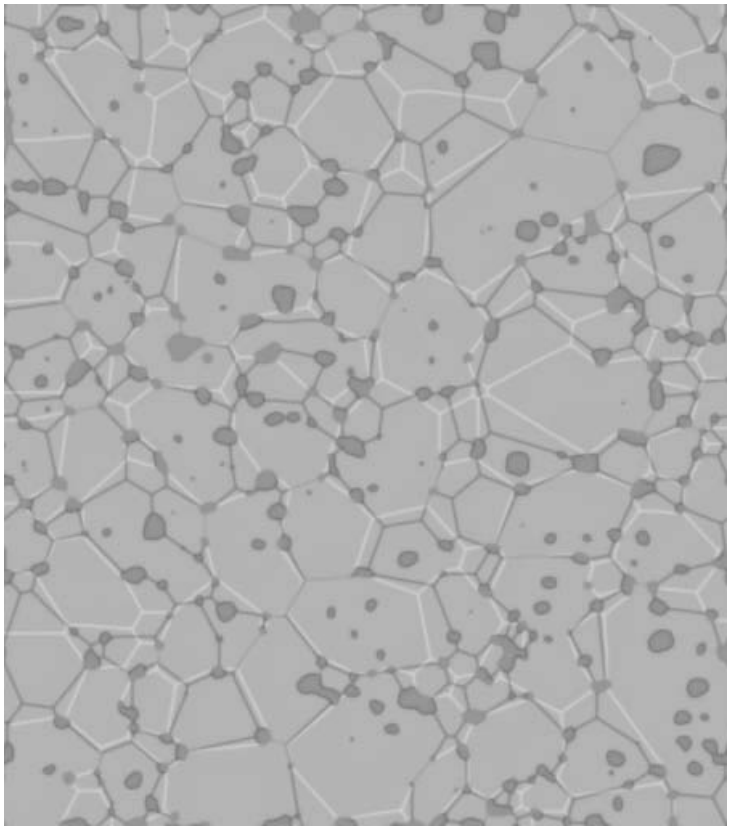

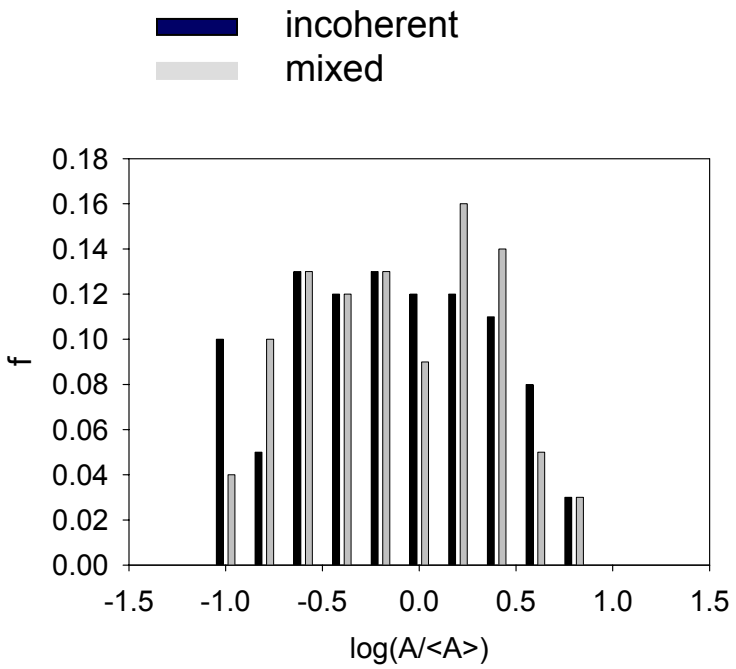

Phase field model *uniquely* capable of capturing important features of microstructure:

- **Grain and phase boundary character and coherency**
- **Size and spatial distribution of precipitates**
- **Time evolution of precipitates (dissolution and coarsening)**

Phase Field Model of Dislocations at Mesoscale

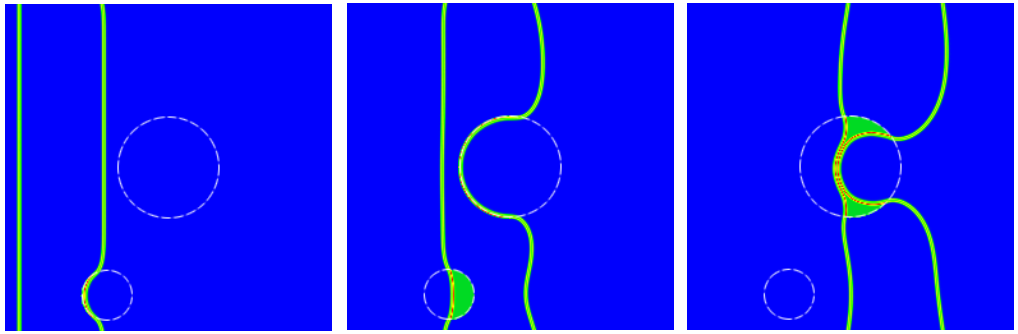

Dislocation-precipitate interaction

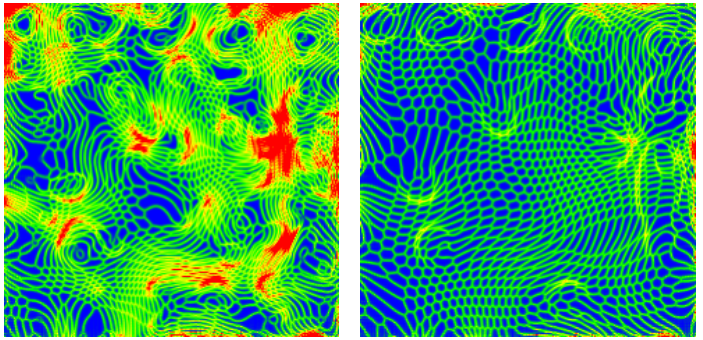

Formation of dislocation network

Benefit of the field description:

1. **Arbitrary poly-domain microstructure and dislocation configuration**
2. **Computational cost insensitive to the complexity of the microstructure**

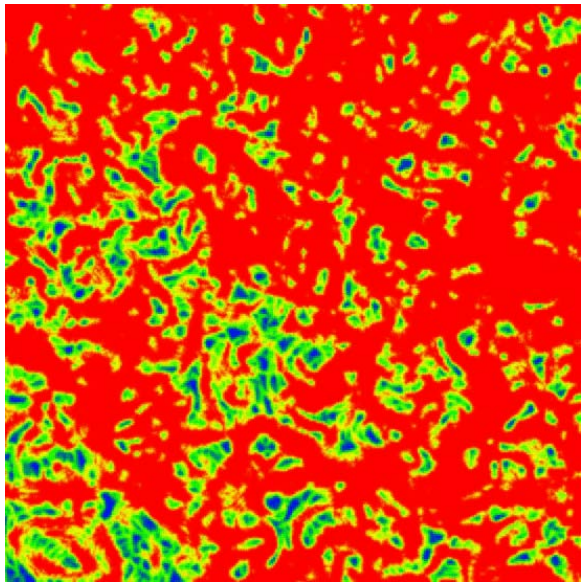

Shen & Wang, Acta Mater 51(2003)2595; *ibid* 52(2004) 683; Jin, Artemev and Khachaturyan, Acta Mater. 49 (2001) 2309

Limitations of Conventional Phase Field Method

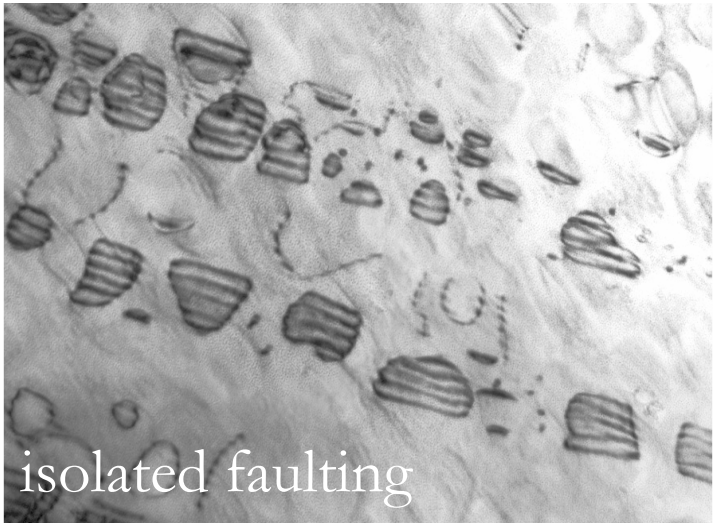

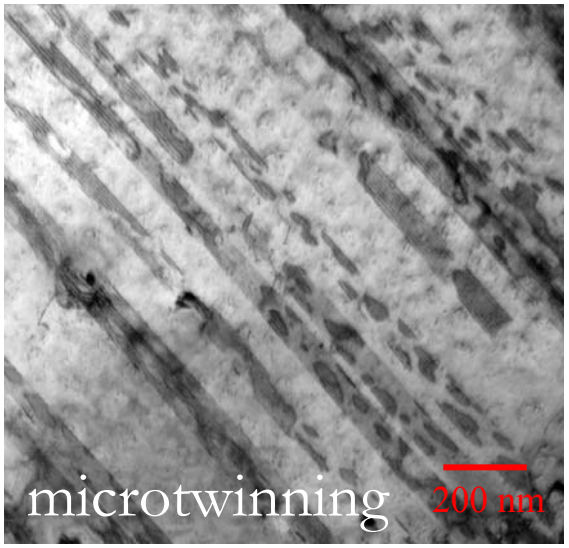

B. Viswanathan and M. J. Mills

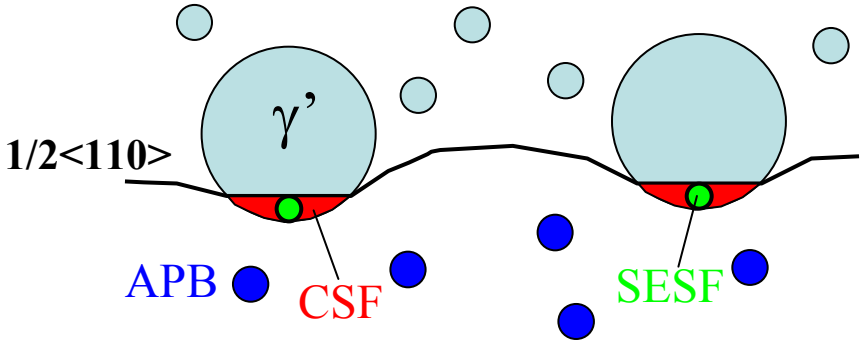

γ' cutting and Shockley partial nucleation for isolated faulting in Ni-base disk alloy

Micromechanisms of creep deformation of Ni-base superalloys

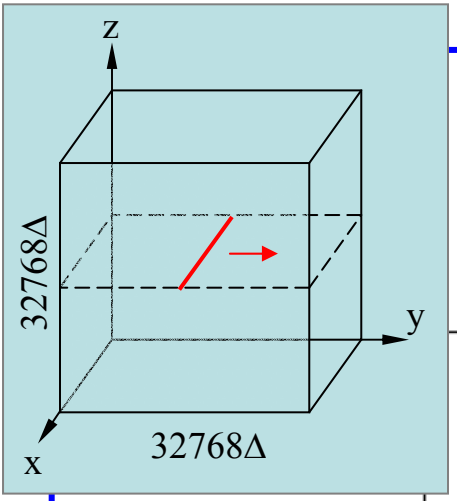

Dissociated dislocation core structure

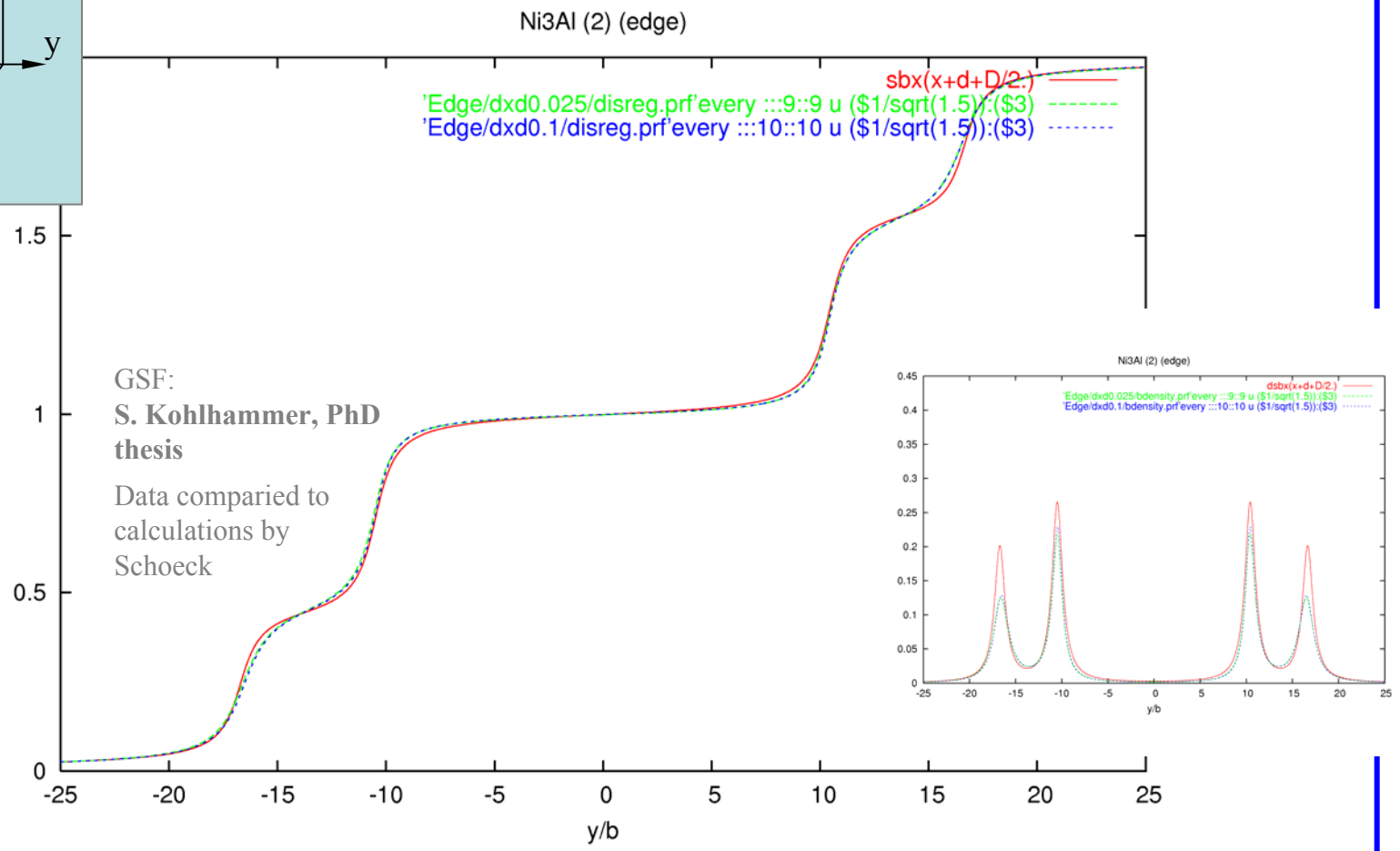

Mechanisms of isolated faulting

Model proposed by Decamps et. al. (1987, 1991, 1994) and Mukherji et. al. (1991):

- Precipitate sheared initially by 1/2<110> forming an APB
- APB transforms into SISF/SESF via nucleation on APB of 1/6<112> partial

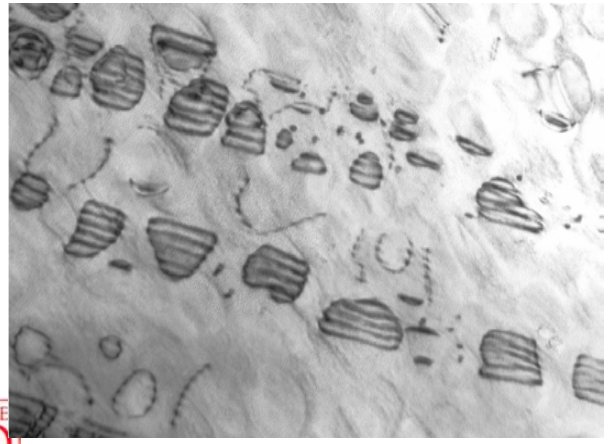

B. Viswanathan and M. J. Mills

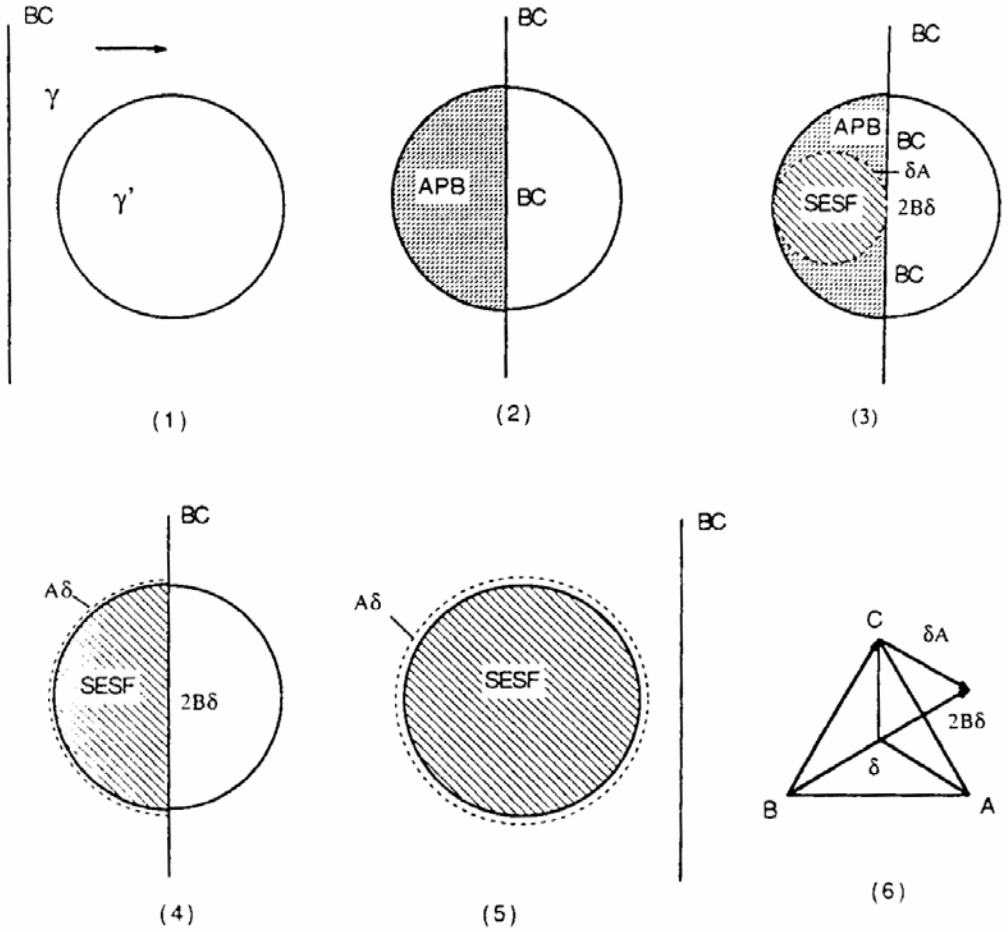

Nucleation of SISF on APB

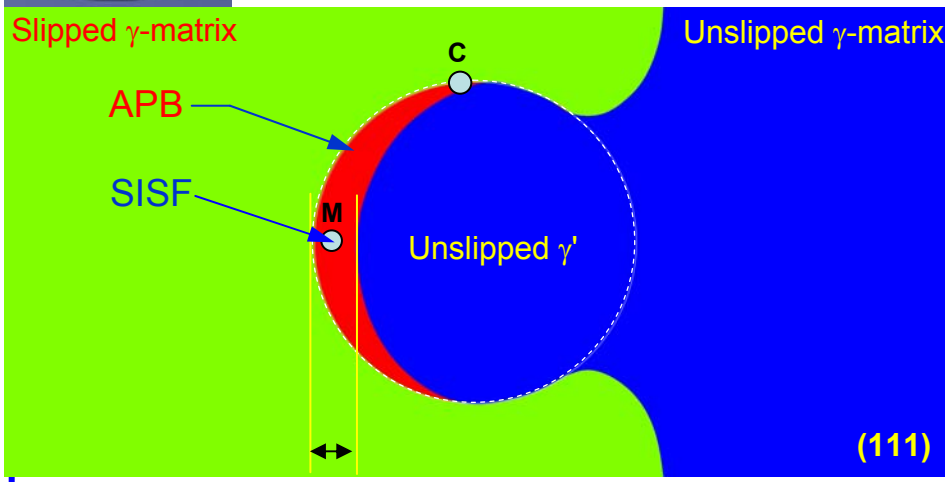

19nm

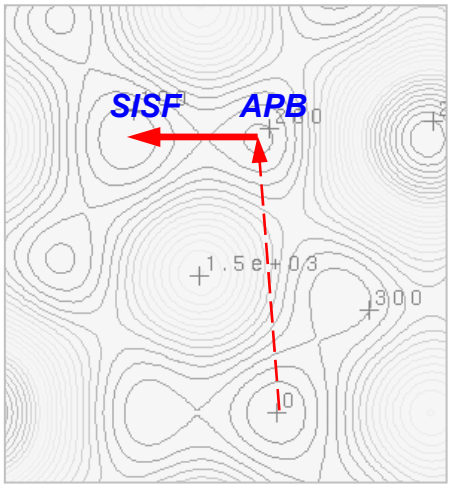

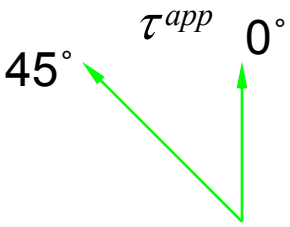

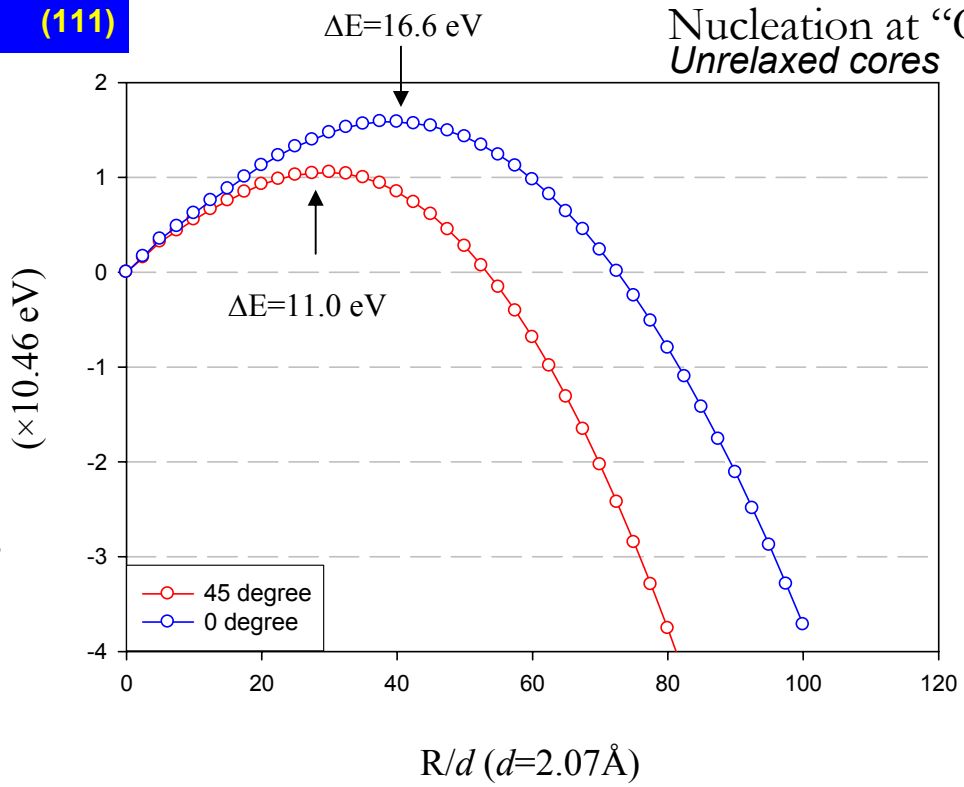

Nucleation of SESF on CSF

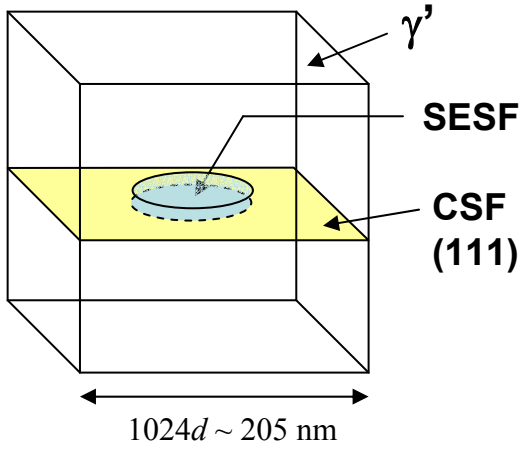

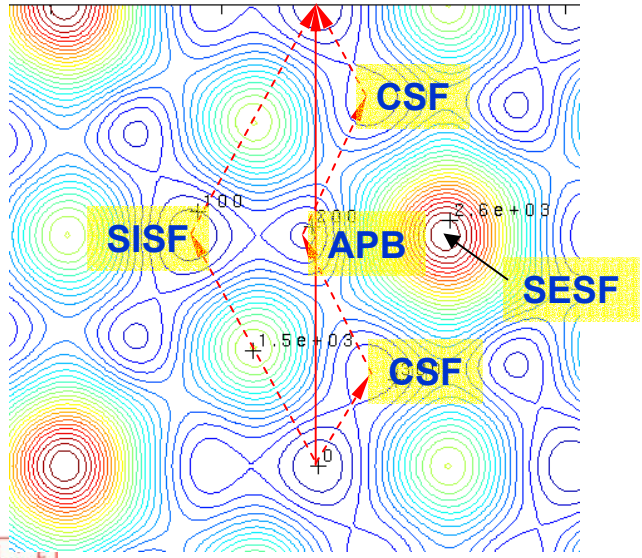

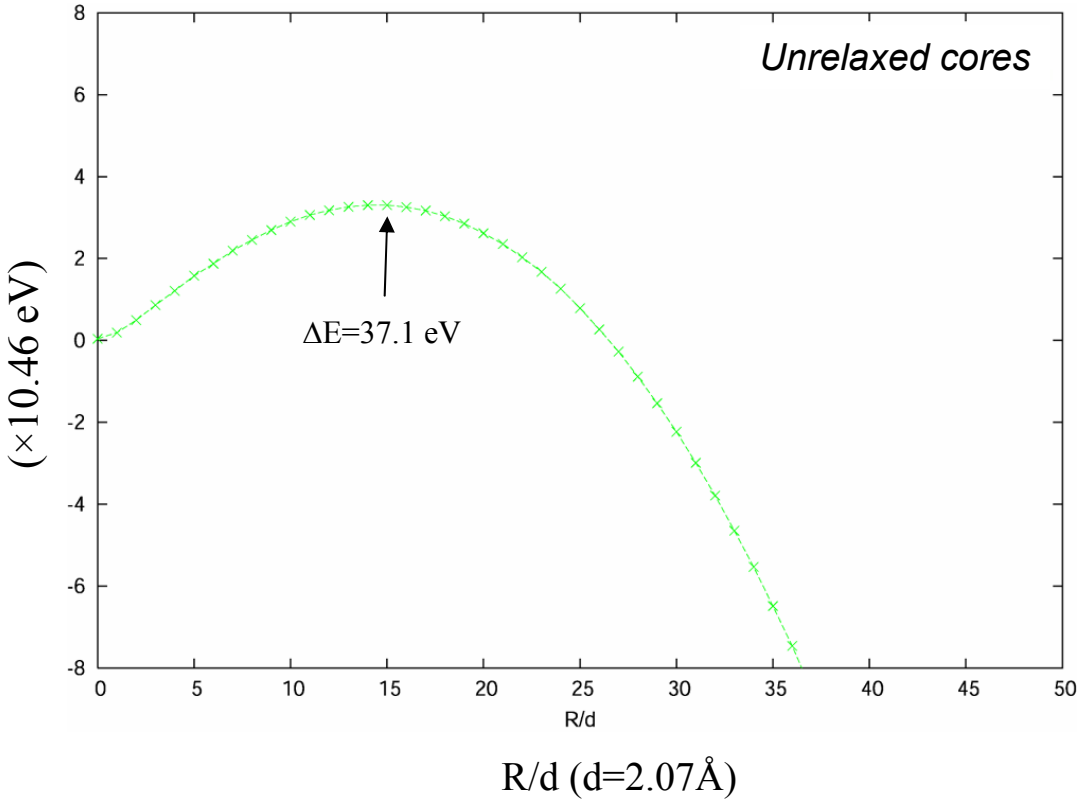

R/d (d=2.07Å)

Multiplane Generalized Stacking Fault Energy

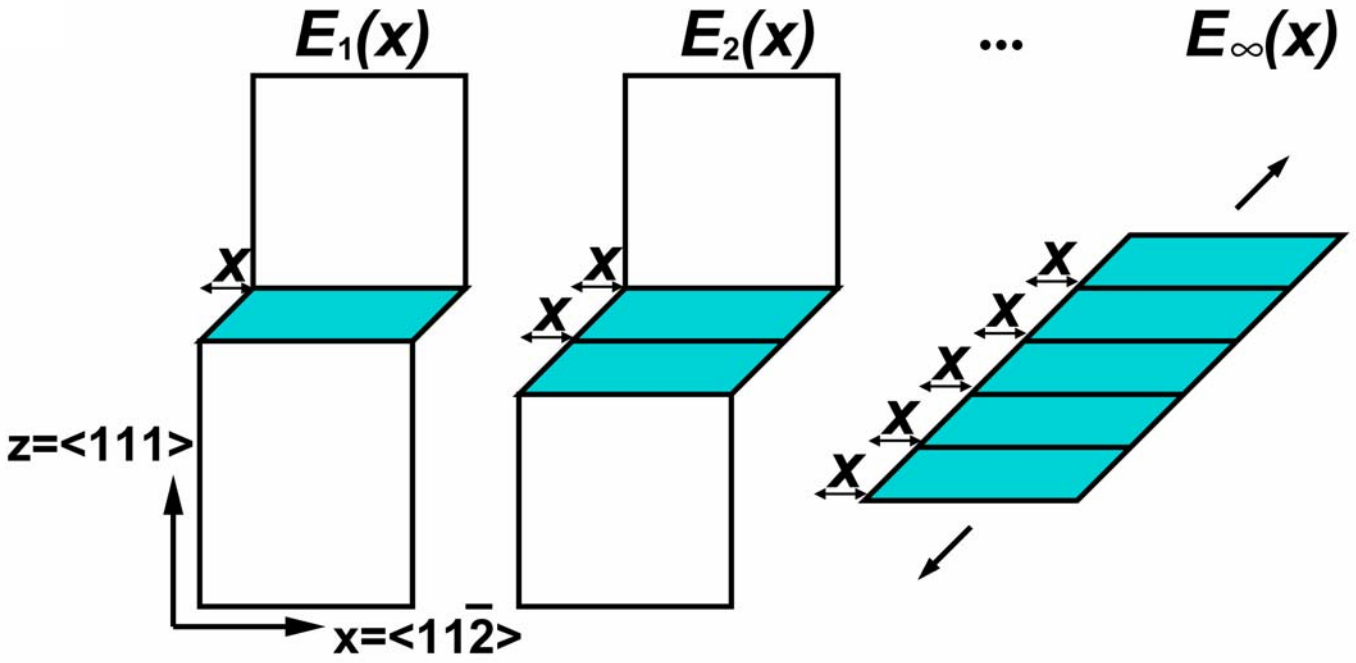

$$\gamma_n(x) \equiv \frac{E_n(x)}{nS_0}, \qquad n = 1,2,3,\ldots,\infty$$

Ju Li (OSU)

Ni_3Al pseudo-twinning *m*GSF

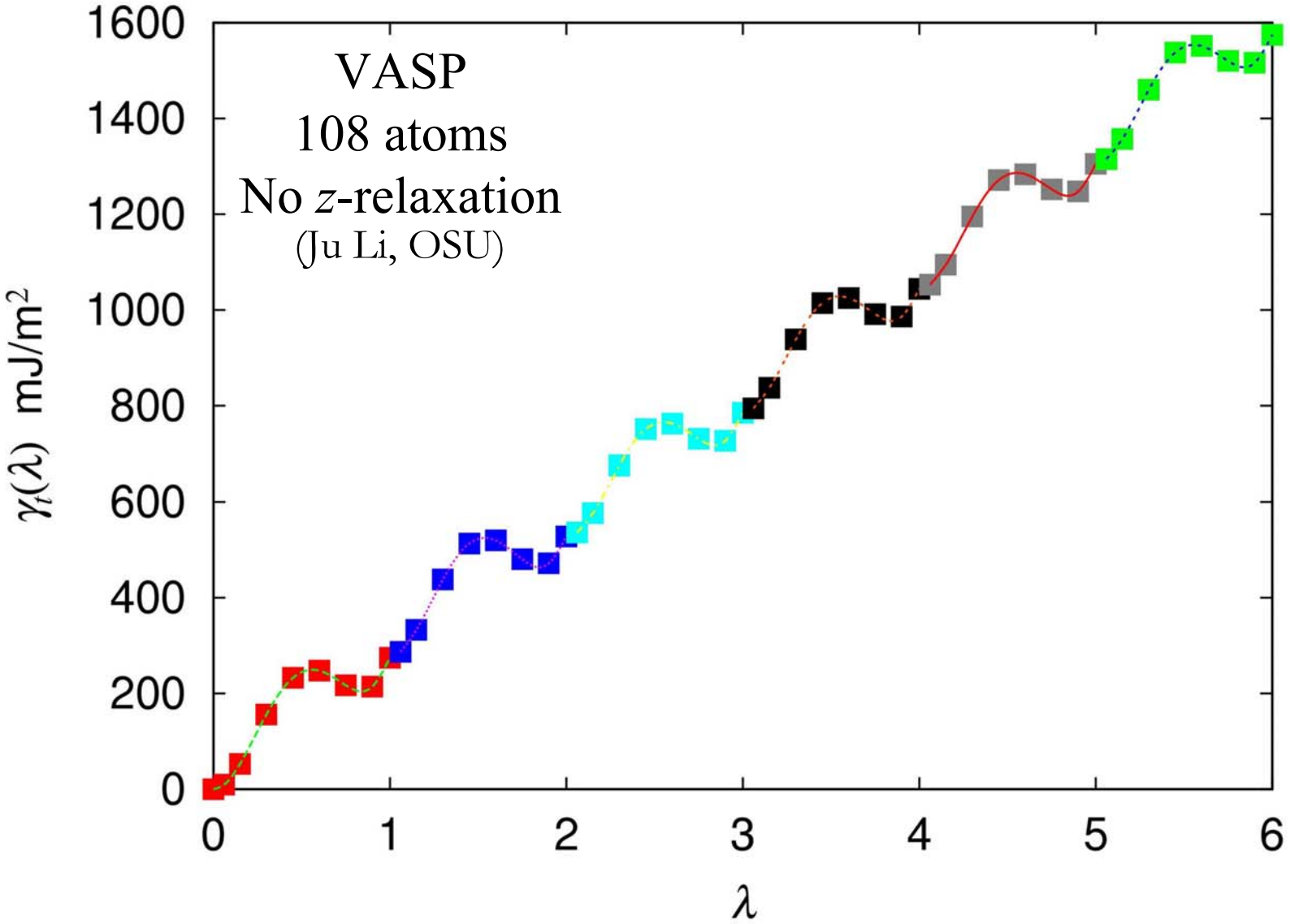

unting for Re-ordering

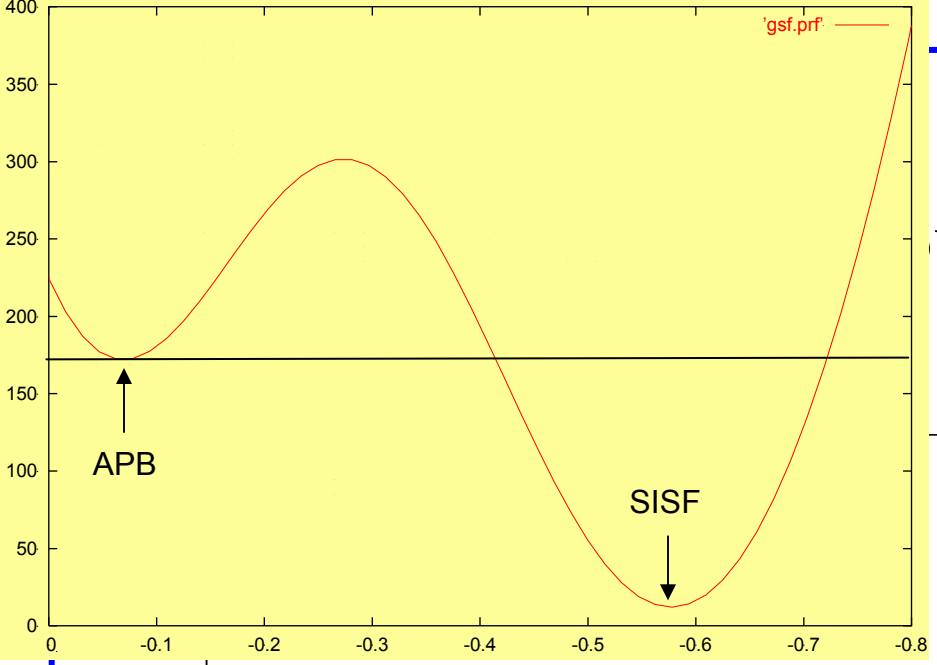

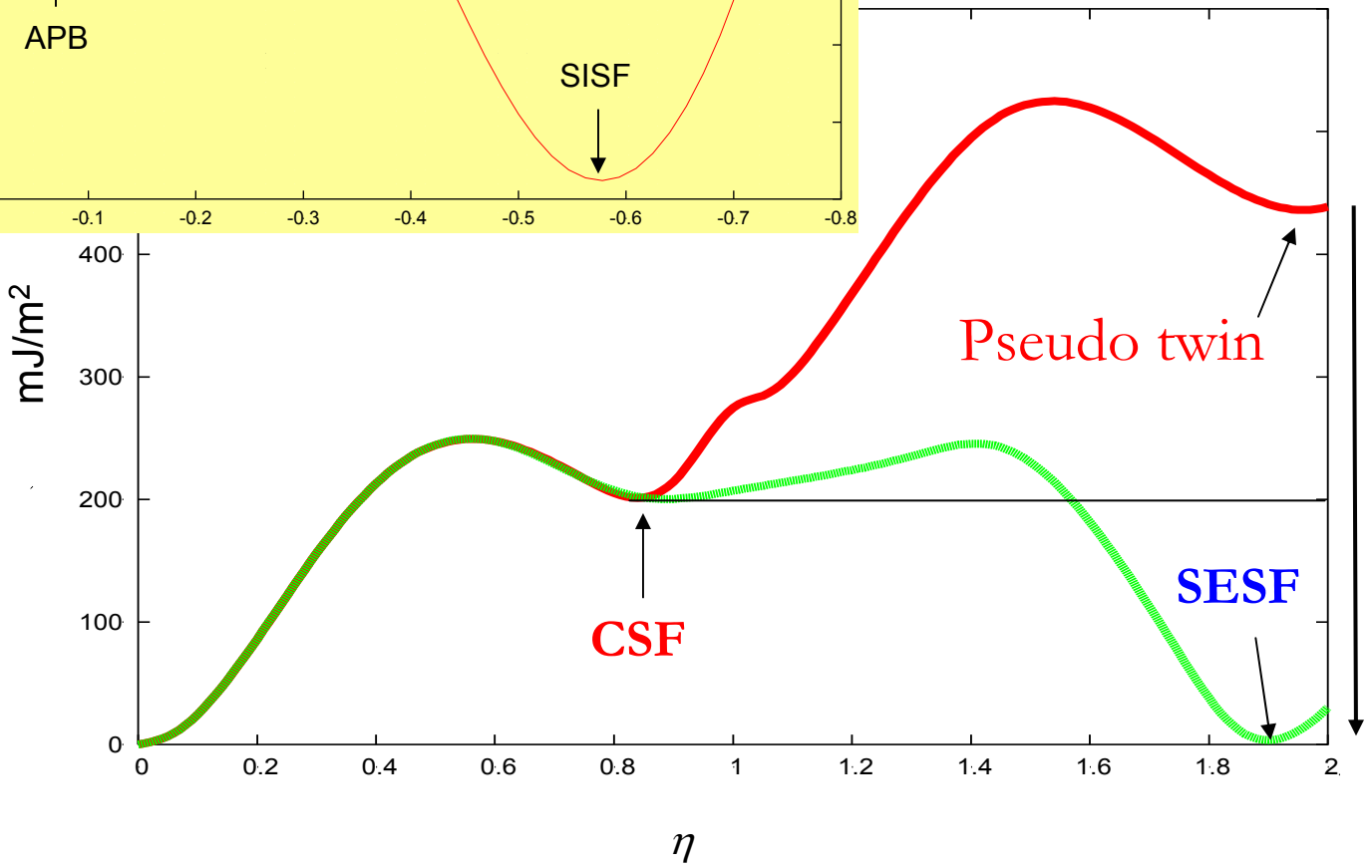

Chemical re-ordering lowers the effective GSF surface

Ju Li (OSU)

Reduced barrier height due to

(a) immediate reordering; (b) relaxed dislocation configurations; (c) applied stress

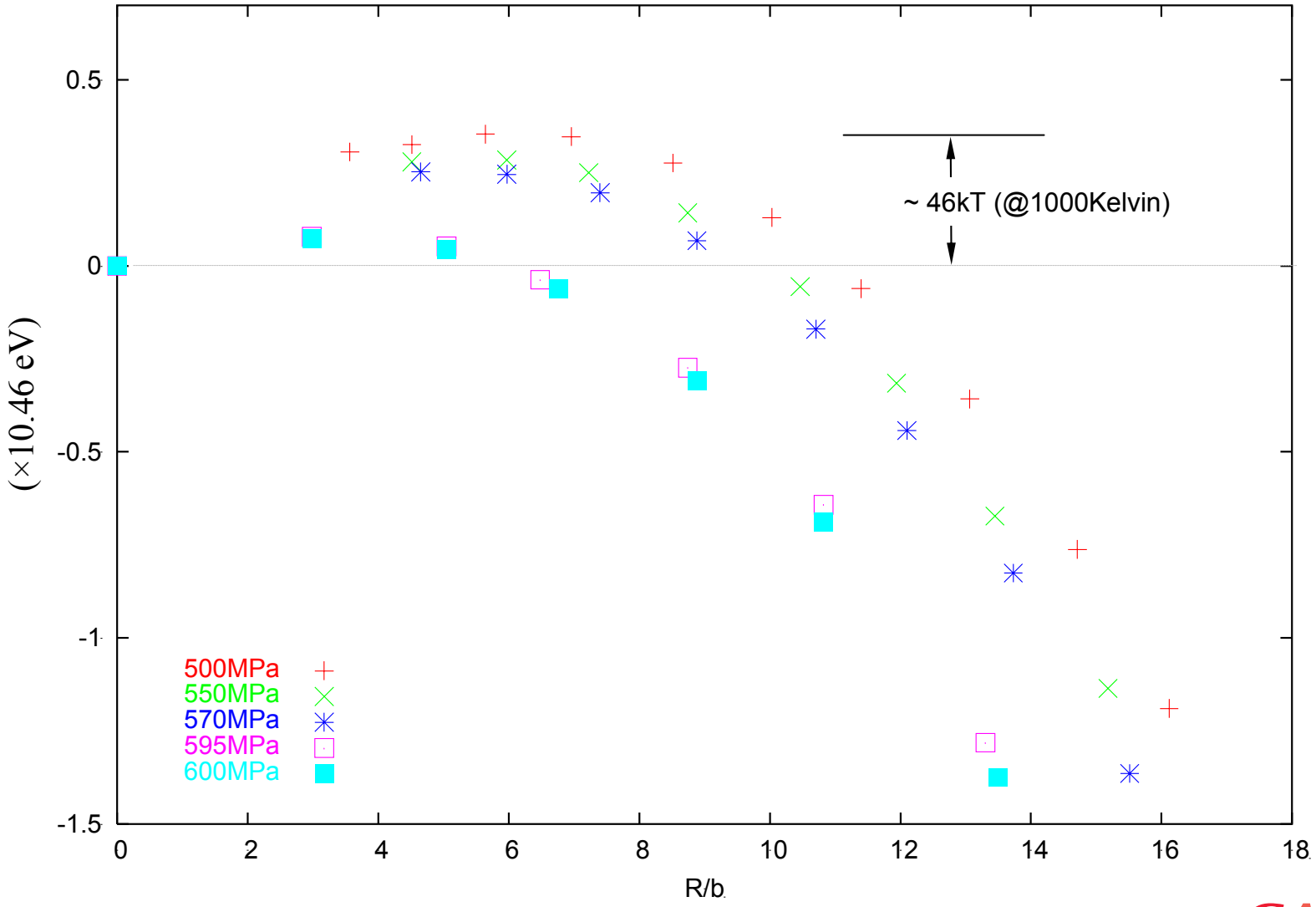

NEB Calculations

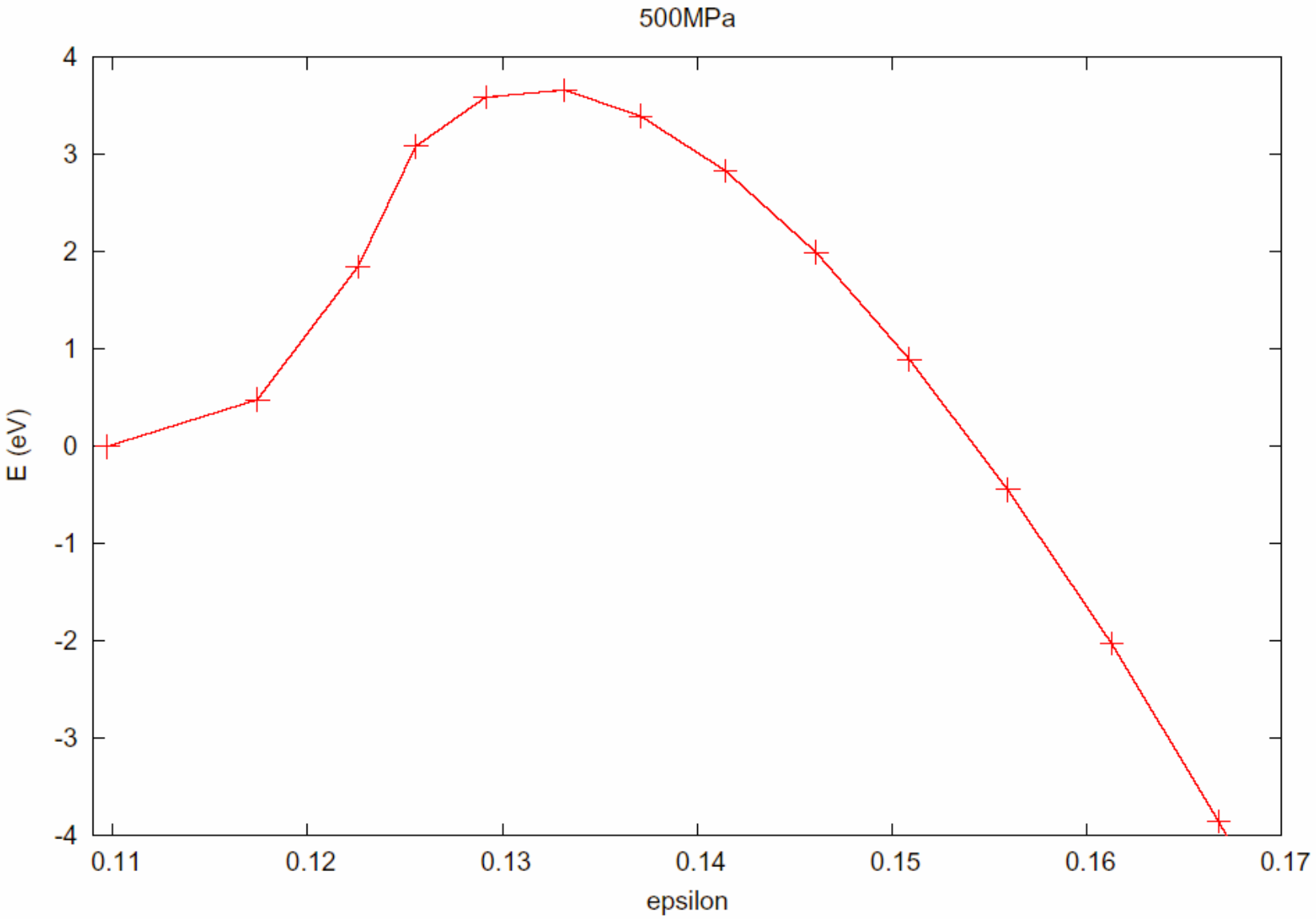

NEB Calculations of Activation Energy as Function of Applied Stress

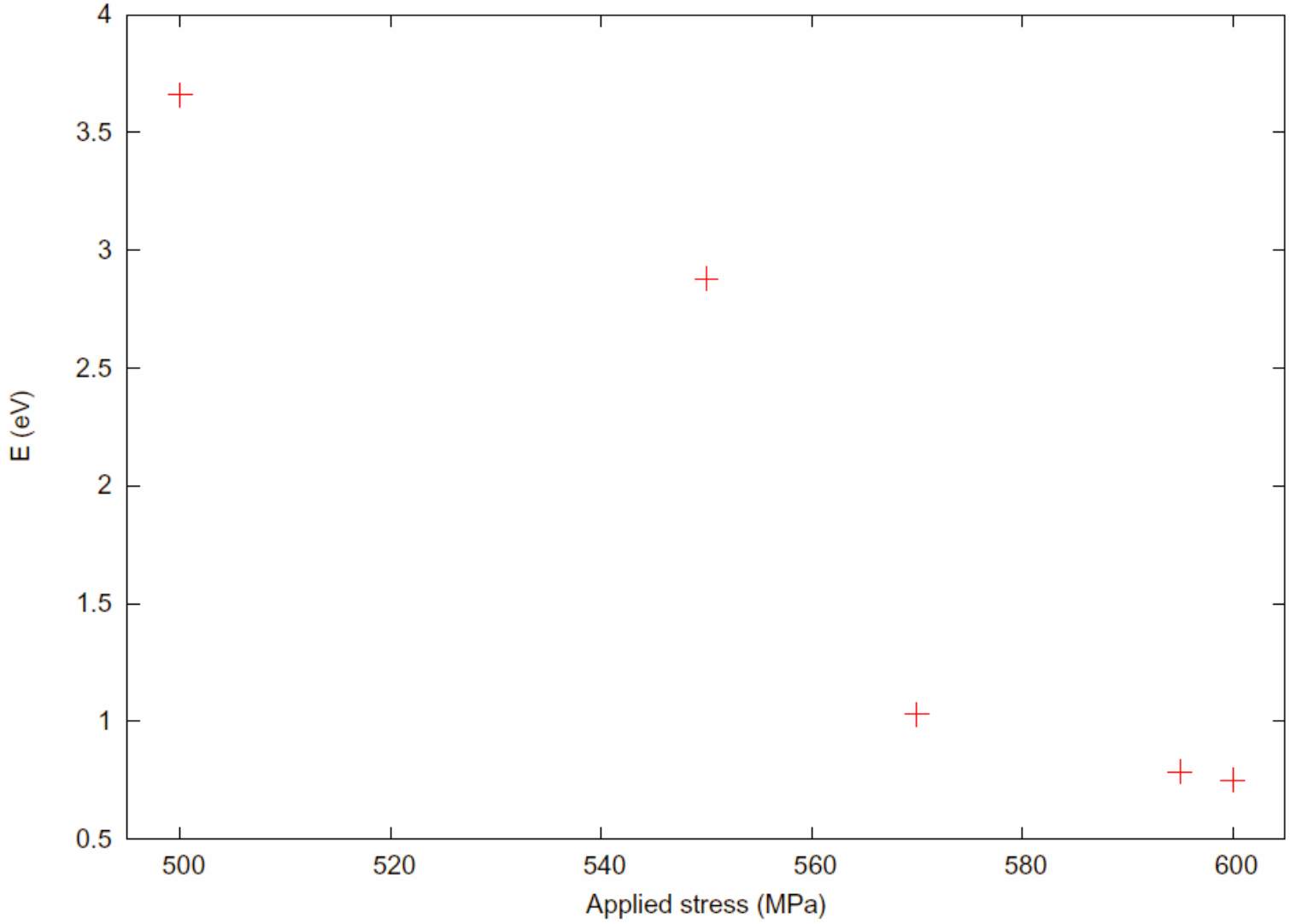

a_2 Basal Slip Compression

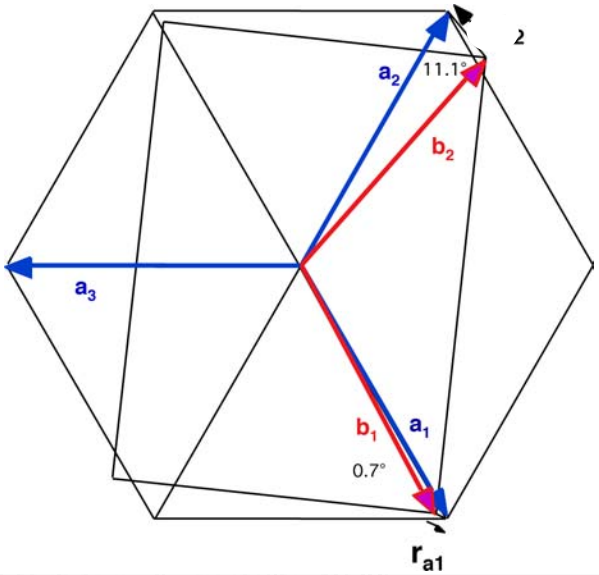

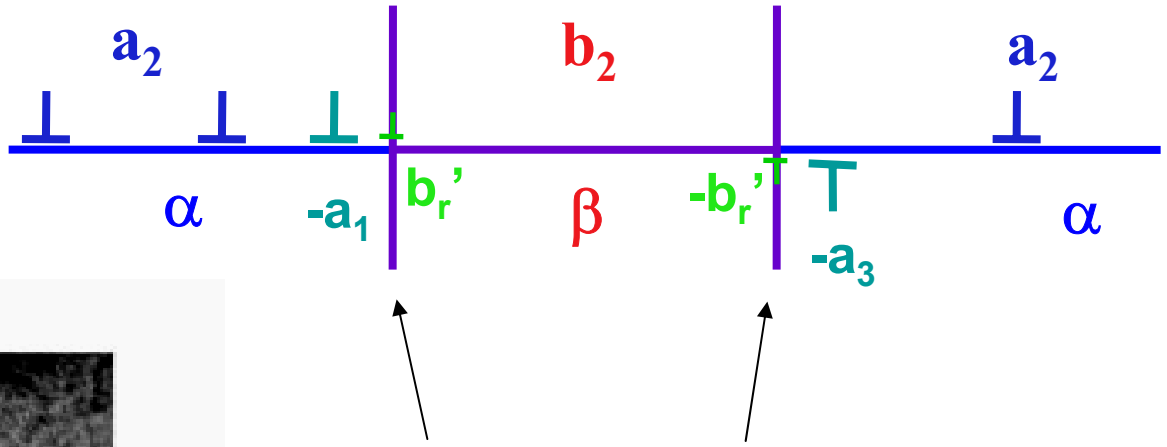

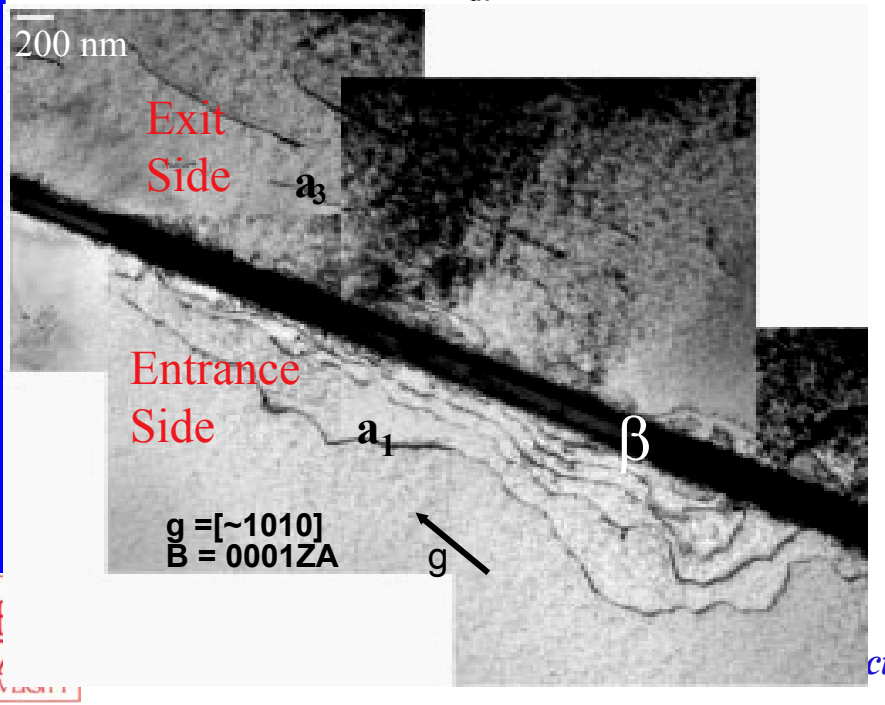

- Accumulation of residual *matrix* dislocations causes increased strain hardening

GSFs

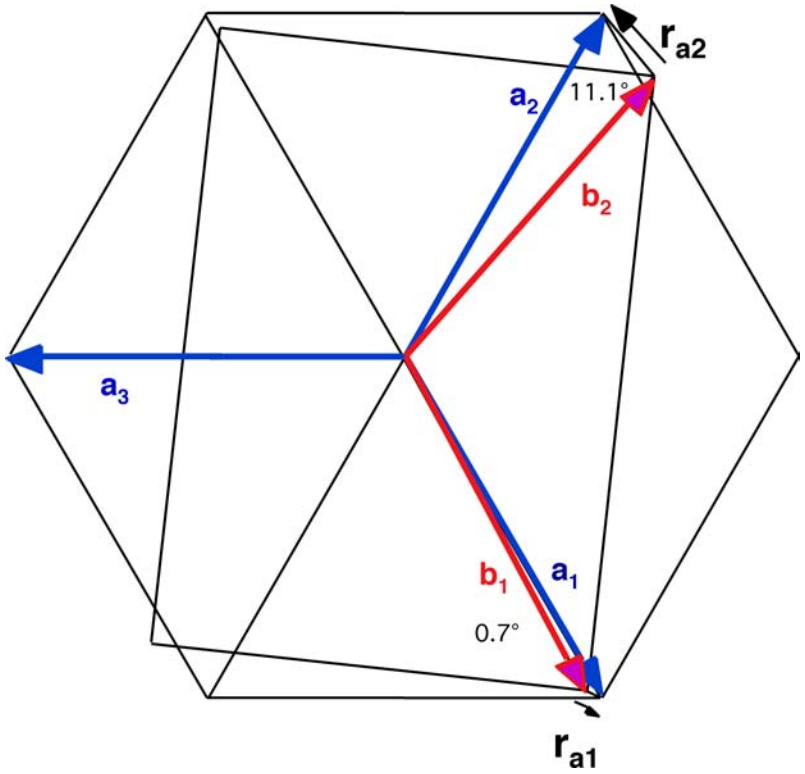
r_{a2}
a_2
11.1°
b_2
a_3
b_1
a_1
0.7°
r_{a1}

HCP

BCC

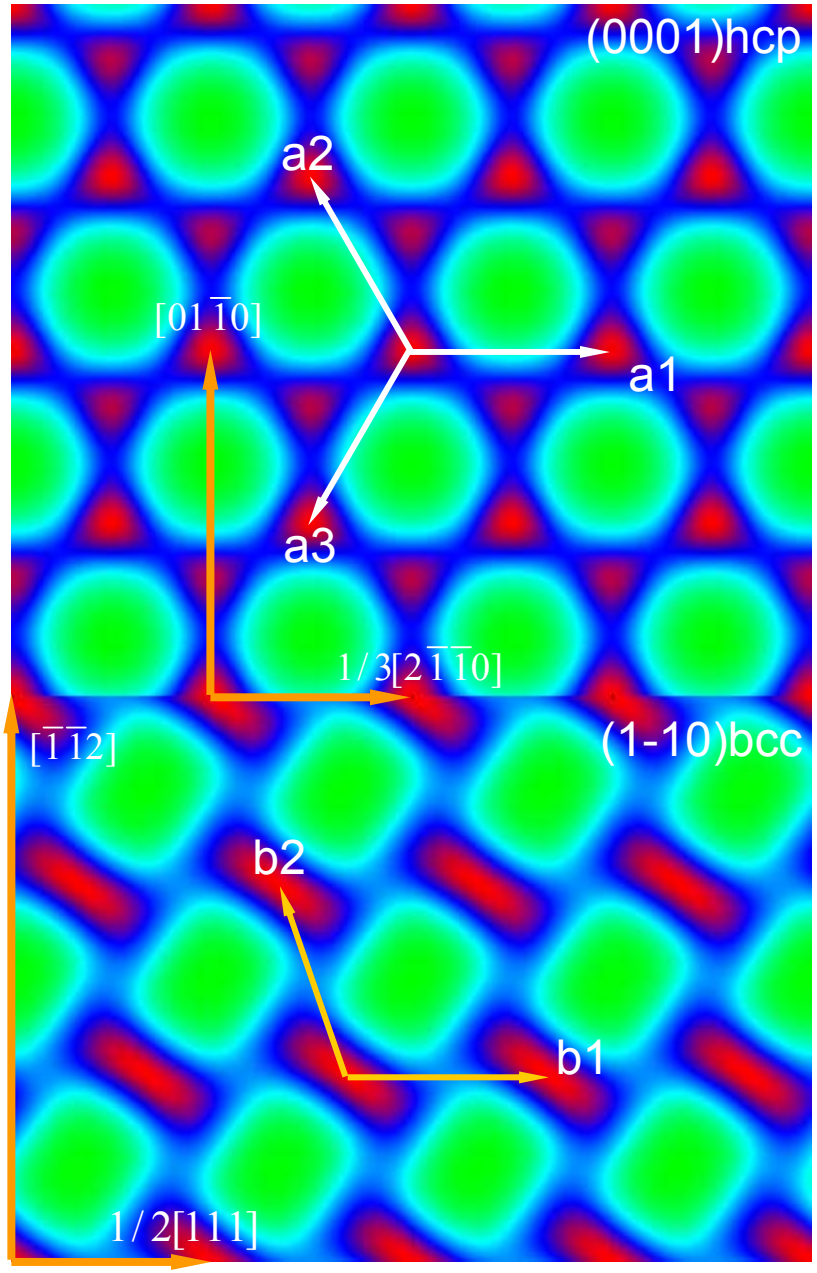
(0001)hcp
a2
[01$\bar{1}$0]
a1
a3
1/3[2$\bar{1}\bar{1}$0]
[$\bar{1}\bar{1}$2]
(1-10)bcc
b2
b1
1/2[111]

animation

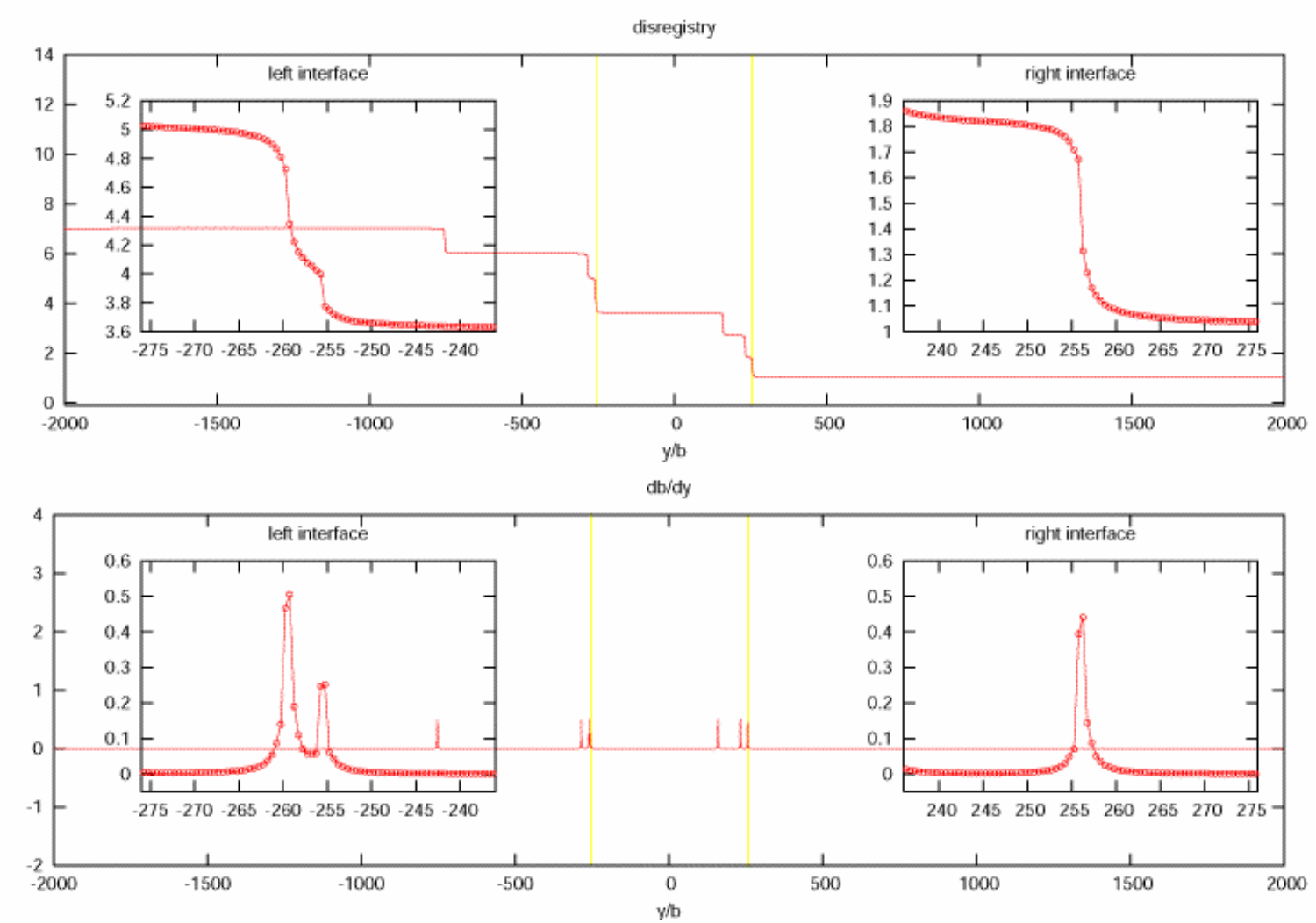

b1=1.0 b2=0.9 b1=1.0

Update from Chen

Summary

- Phase field modeling capabilities at multiple length scales have been developed for coupled microstructural evolution and dislocation process
- At mesoscopic level, 3D quantitative phase field model of microstructure evolution under non-isothermal conditions has been calibrated against experimental study
- At microscopic level, the phase field model has been shown to be a 3D generalization of the Peierls model. Using *ab initio* calculations as inputs, the model has been applied to study deformation mechanisms in Ni-base superalloys and α/β Ti alloys.
- 2D and 3D quantitative models and digital microstructures have been developed, and their usefulness is being evaluated by team member for NN, DMT, MSD tool development.

Mechanisms of Creep in Disk Alloys

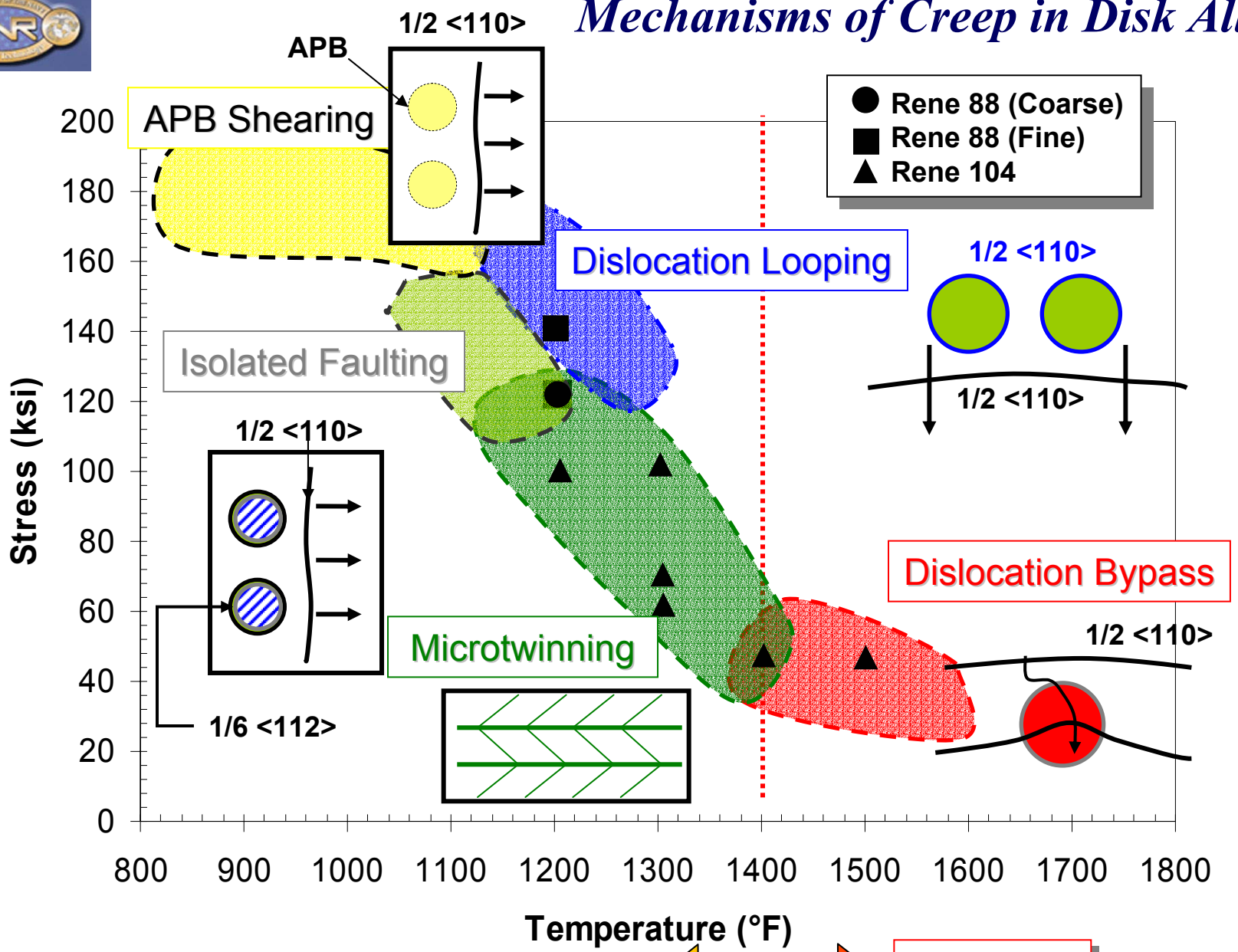

Tertiary γ'

Tertiary γ' Dissolution

Microstructures in Real Engineering Alloys

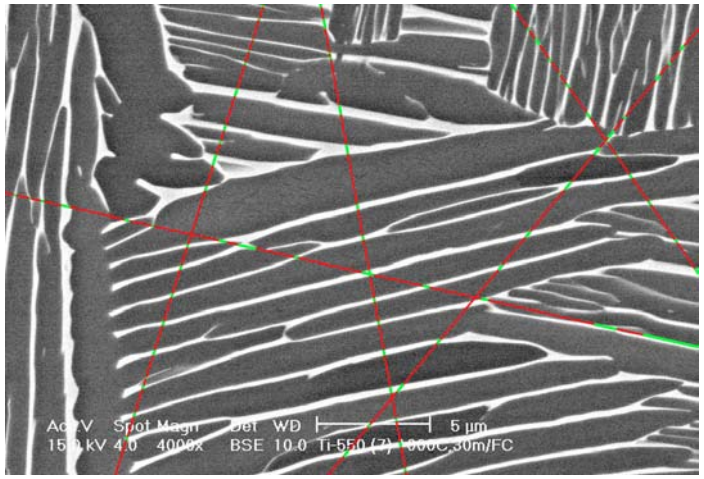

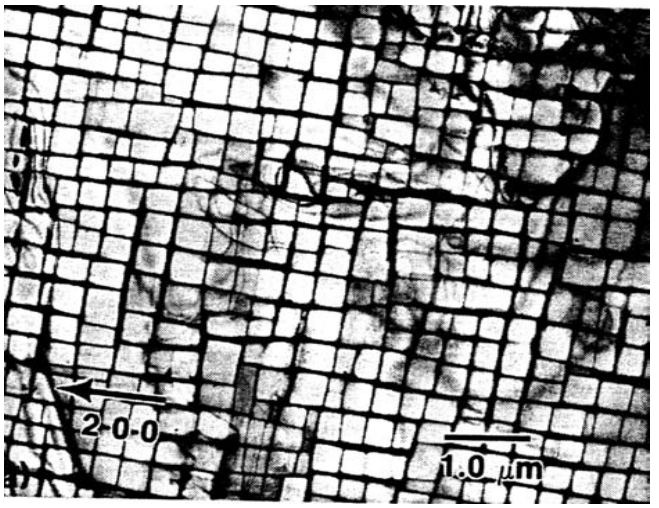

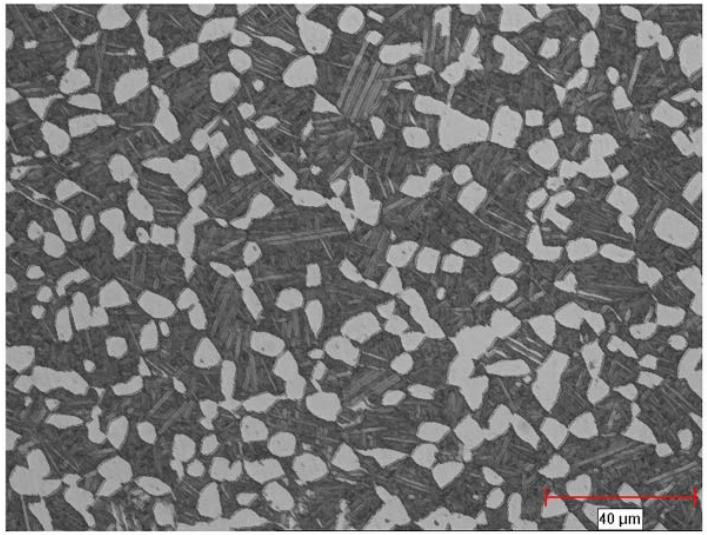

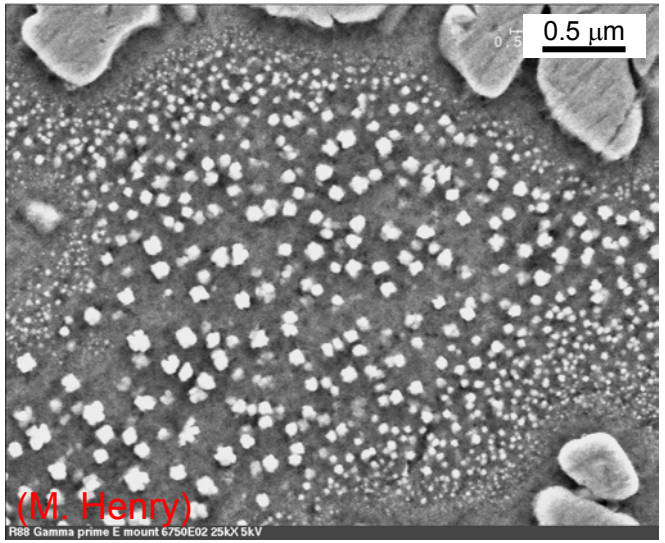

α/β Ti alloy

Ni-base superalloy

Advanced Microstructure Modeling using Phase Field Method

$$\frac{\partial c(\mathbf{r},t)}{\partial t} = \nabla\left(M\,\nabla\frac{\delta F}{\delta c(\mathbf{r},t)}\right) + \xi_c(\mathbf{r},t)$$

$$\frac{\partial \eta_p(\mathbf{r},t)}{\partial t} = -L\frac{\delta F}{\delta \eta_p(\mathbf{r},t)} + \xi_p(\mathbf{r},t)$$

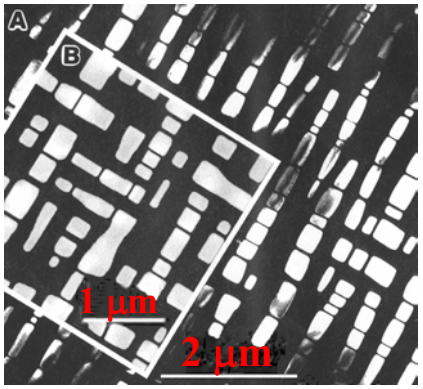

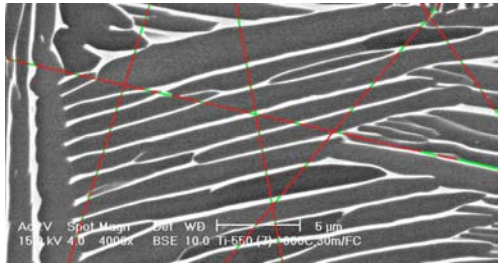

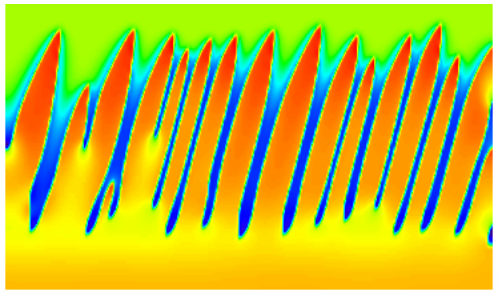

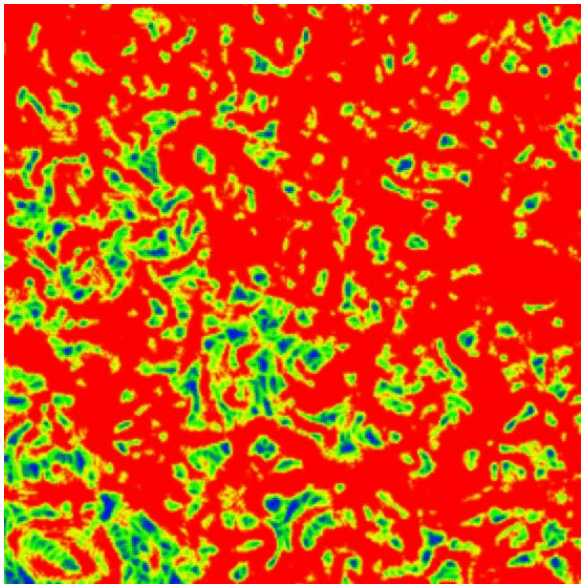

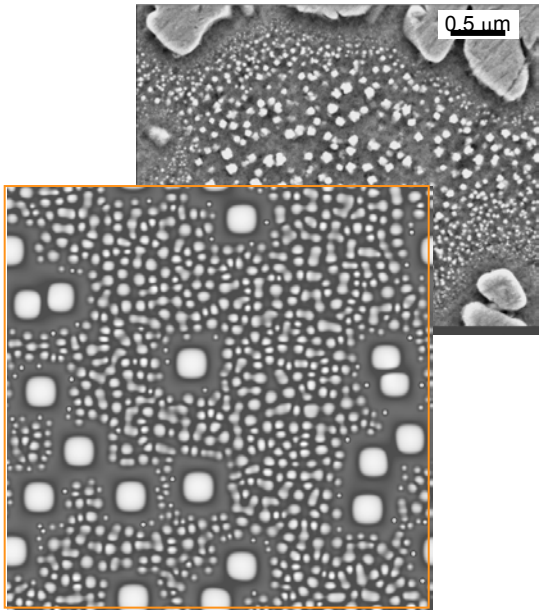

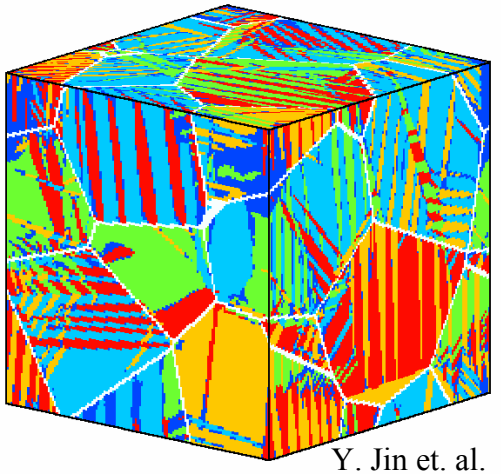

Y. Jin et. al.

The phase field method handles well arbitrary microstructures consisting of diffusionally and elastically interacting particles and defects of high volume fraction and accounts self-consistently for topological changes such as particle coalescence.

Input/Output for Phase Field Modeling of Microstructure

Input

Experimental Data

Atomistic Calculations

Optimizer

Mobility Database

DICTRA

TD Database

Thermo_Calc or PANDAT

Kinetic description

Thermodynamic description

Interface Properties

Elastic Properties

GSF or γ-surfaces

Other properties

Chemical Diffusivity of Al

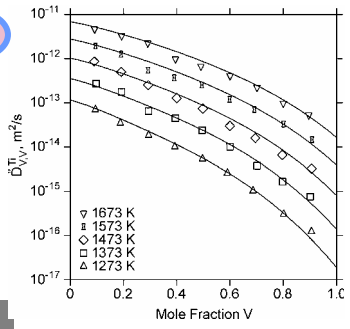

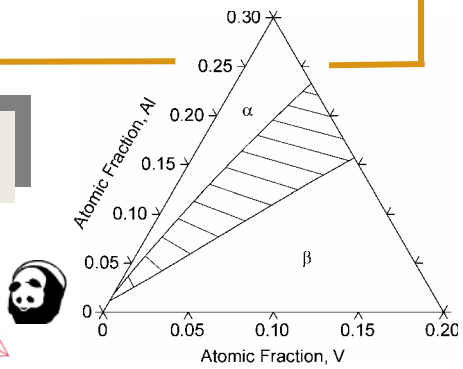

Output

Digital Microstructure to MDT

Phase Field Model

Micro.-Disl. Interaction Model

Constitutive equations for MNN and MSDM training or direct design applications

Dislocation – Microstructure Interaction Modeling

Relevant mechanisms informed by experimental study

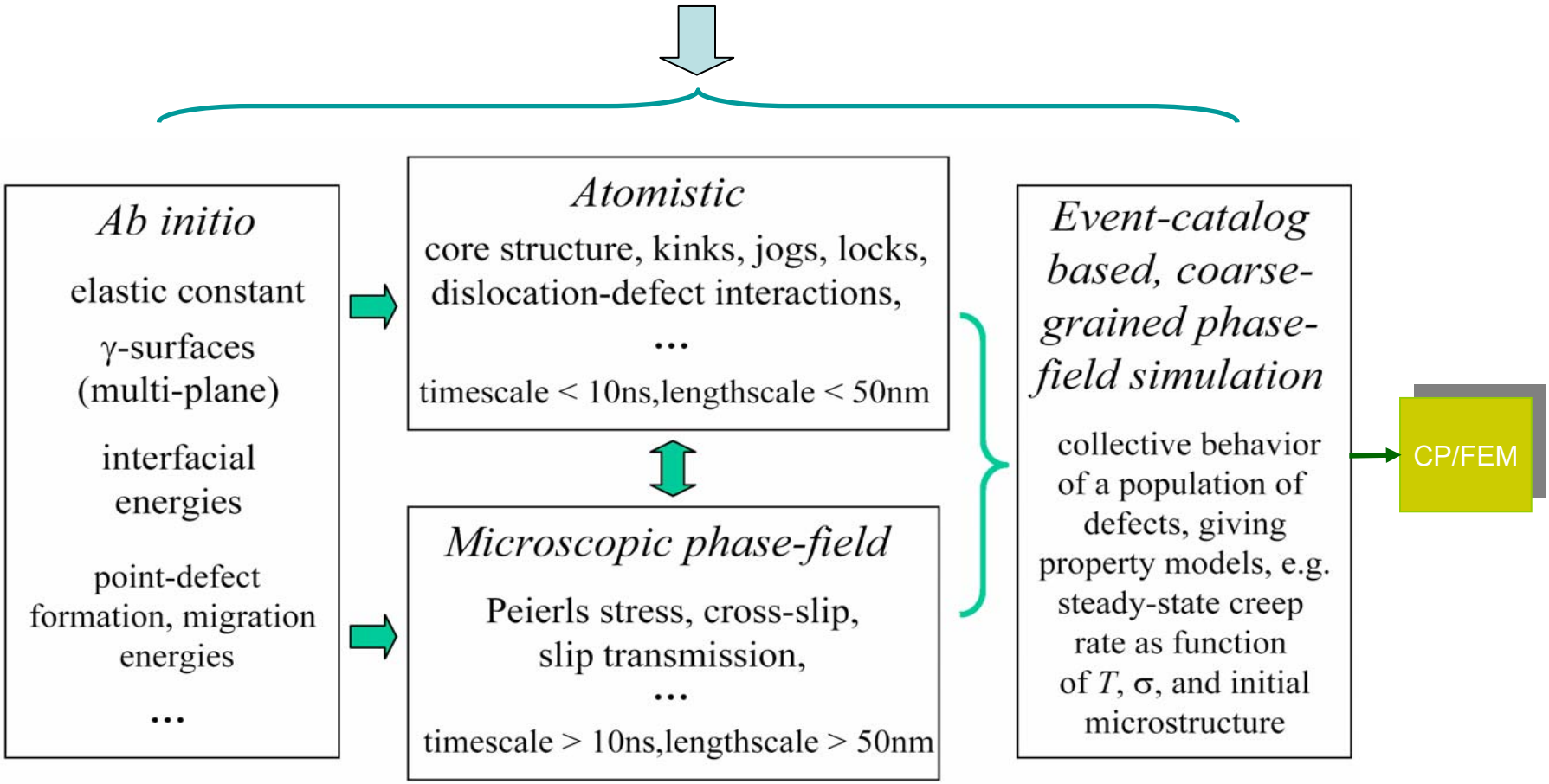

Requirements and Challenges

- Quantitative prediction of detailed microstructural features including precipitate morphology, spatial arrangement and anisotropy
  - at the same level of complexity as experimental observations
  - at the experimentally relevant length and time scales
- Multi-component, multi-phase, and polycrystalline
- Very complex microstructural features:
  - high volume fraction of precipitates
  - strong anisotropy and spatial correlation
  - elastic interactions among precipitates
- Coupling between precipitate microstructure evolution and plastic deformation (dislocation activities)
- Model robustness and computational efficiency

3D quantitative simulation of Ni-23.27Cr-16.49Co-4.3Al-1.22Ti: Comparison with Exp.

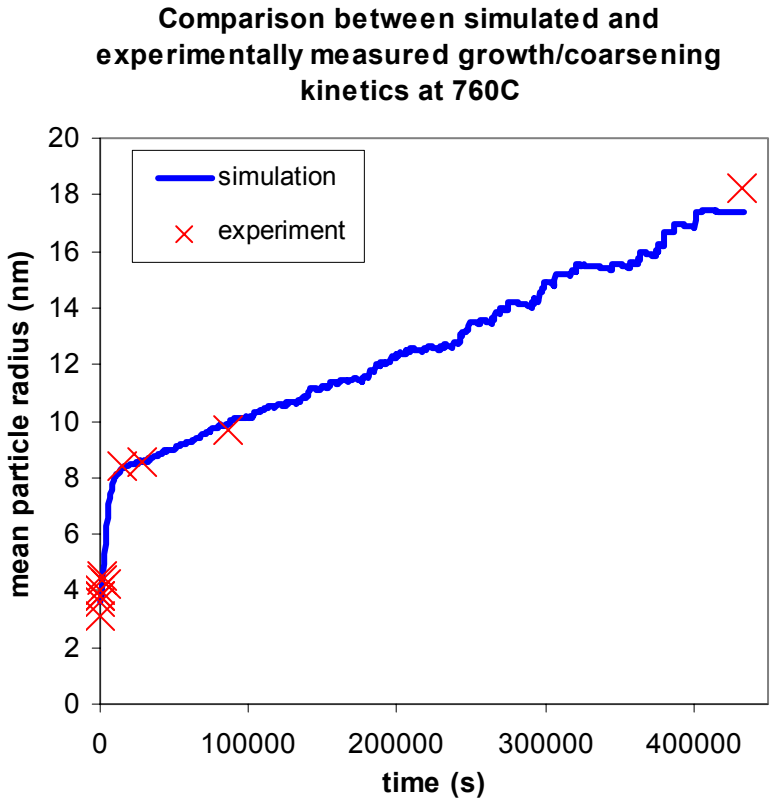

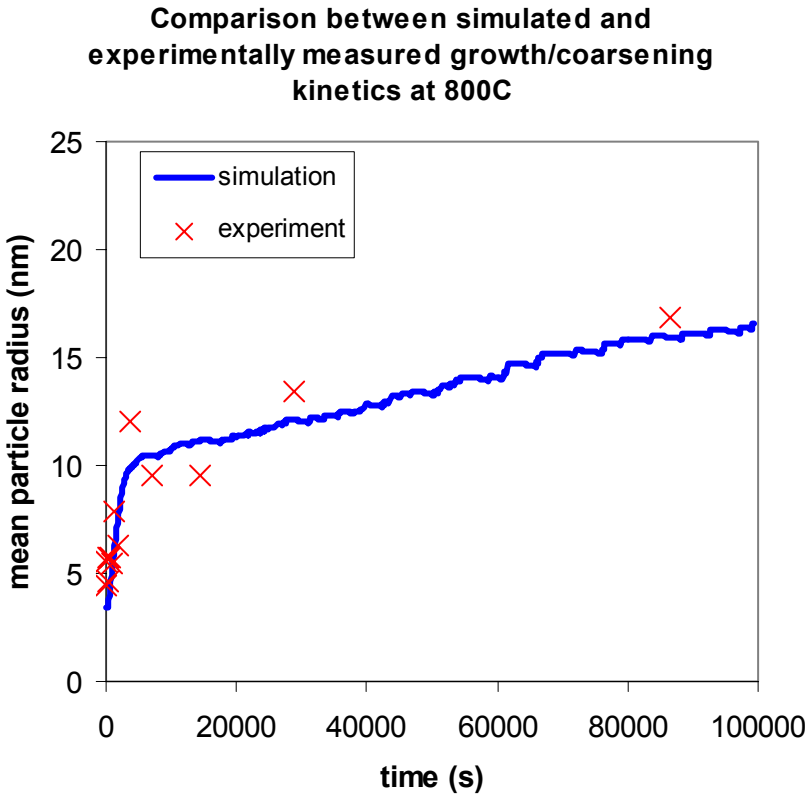

Courtesy of Y. Wen and J. P. Simmons

Formation of γ/γ' Bimodal Microstructure

Phase Field Model of Nucleation

Nucleation Movie I

Nucleation Movie II

Homogeneous Nucleation under Continuous Cooling at 10°C/s

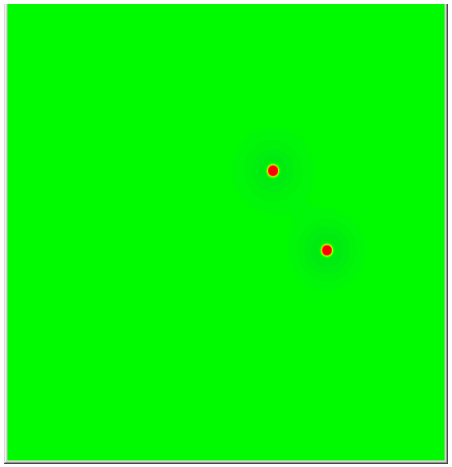

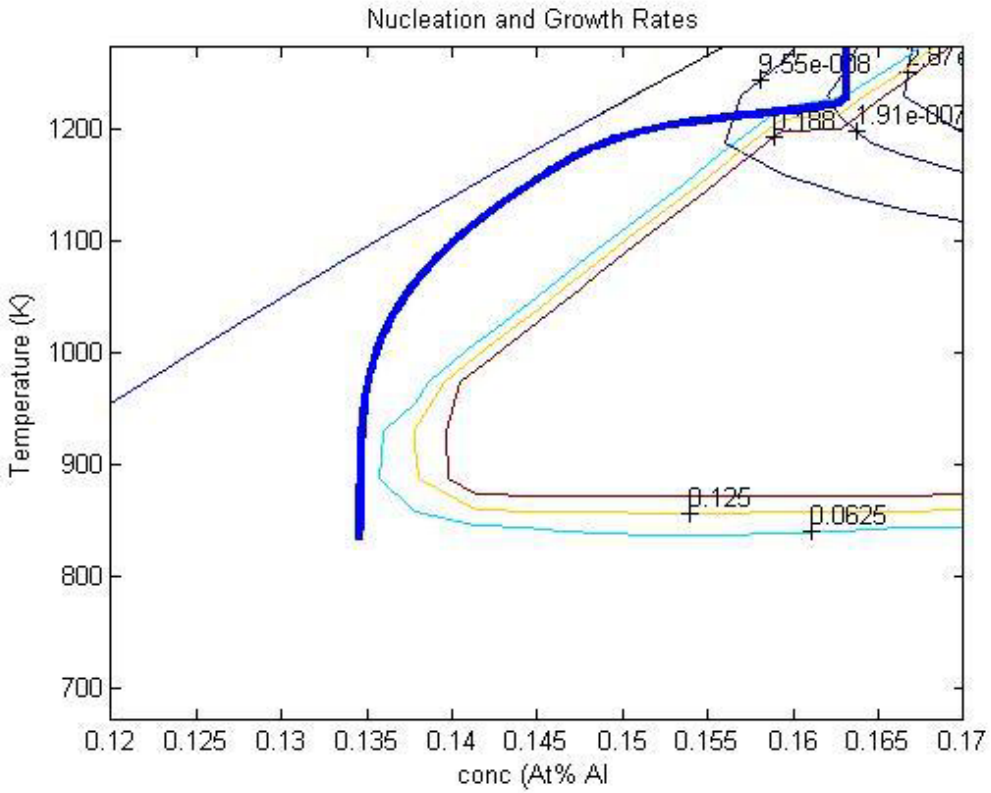

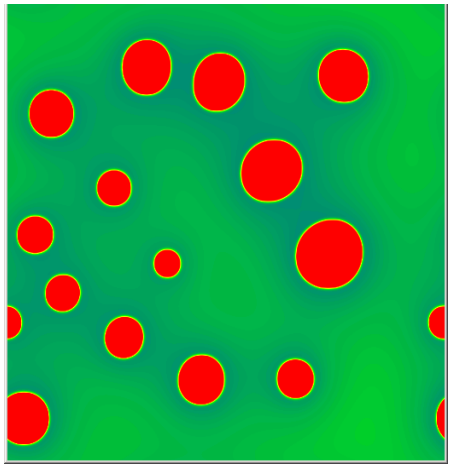

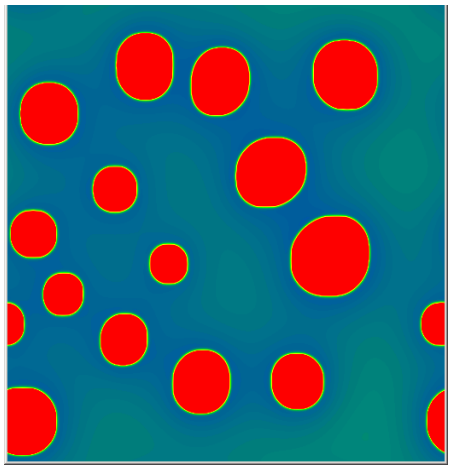

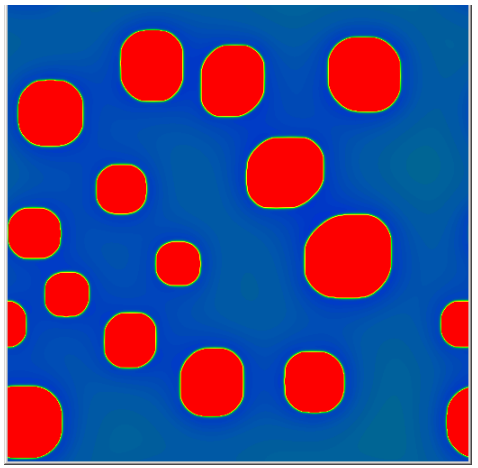

Homogeneous Nucleation under Continuous Cooling at 20°C/s

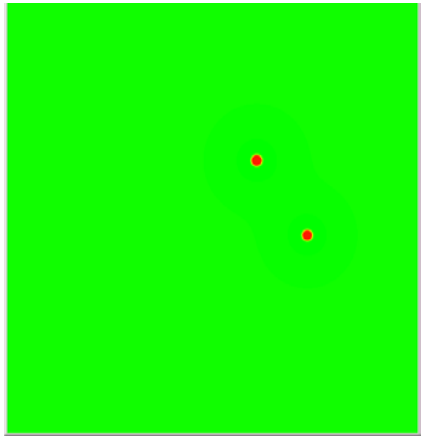

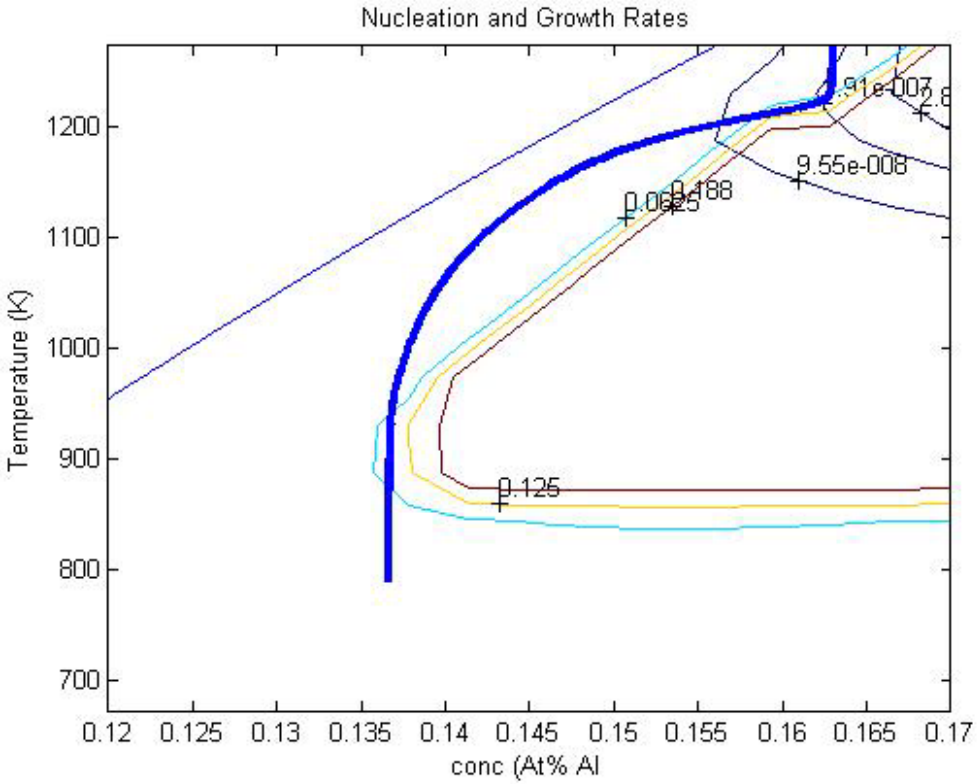

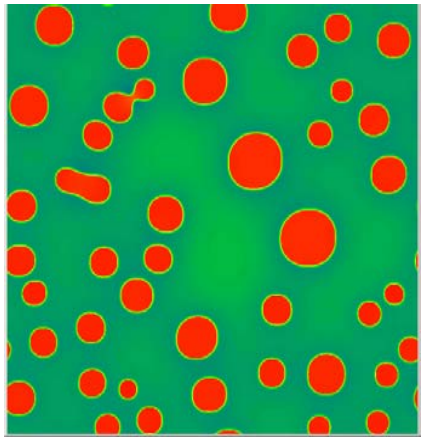

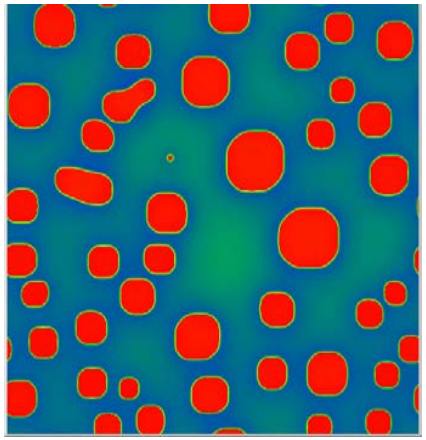

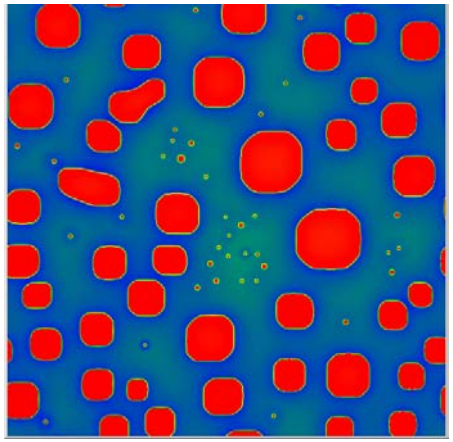

Homogeneous Nucleation under Continuous Cooling at 40°C/s

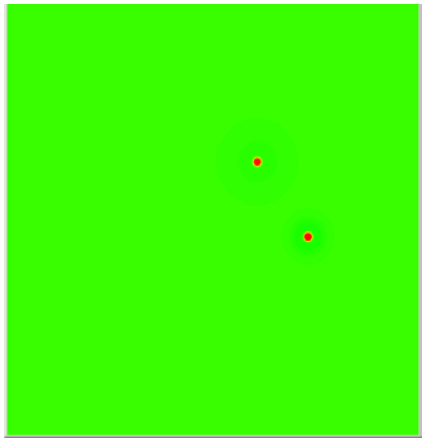

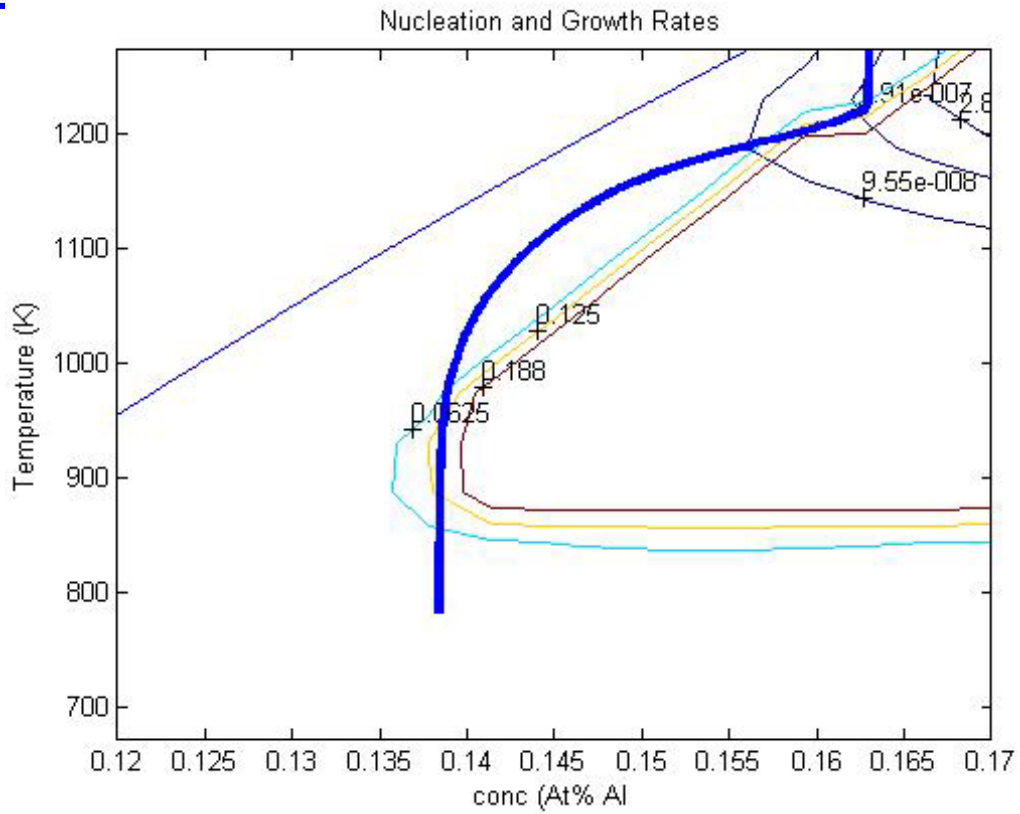

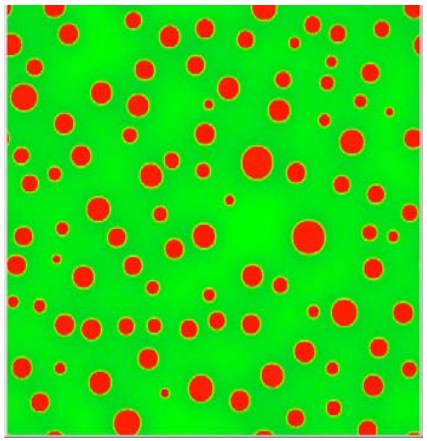

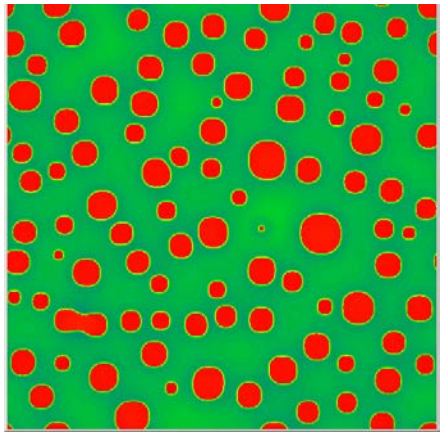

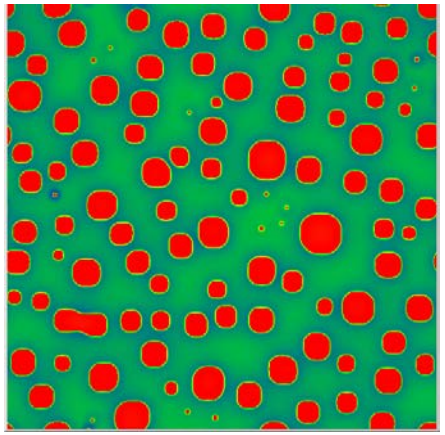

Effect of Alloy Composition

T_{init}= 950C T_{final}= 450C at 10°C/s

C = 0.163

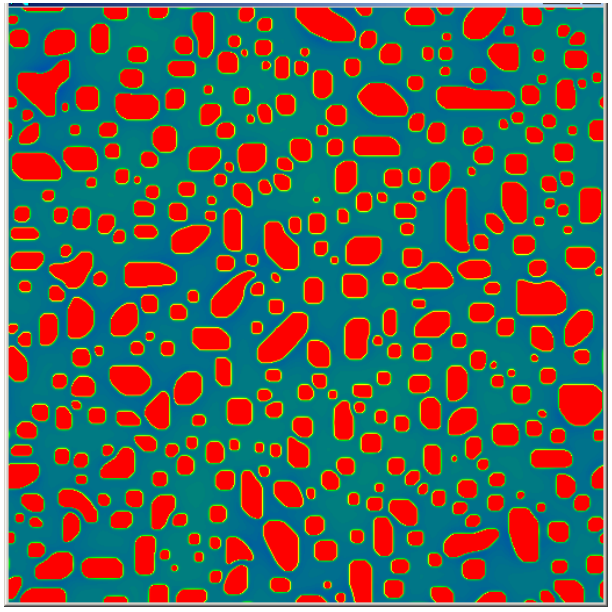

Equilibrium VF (450C) : 44.11%

Final Simulation AF : 42.96%

C = 0.153

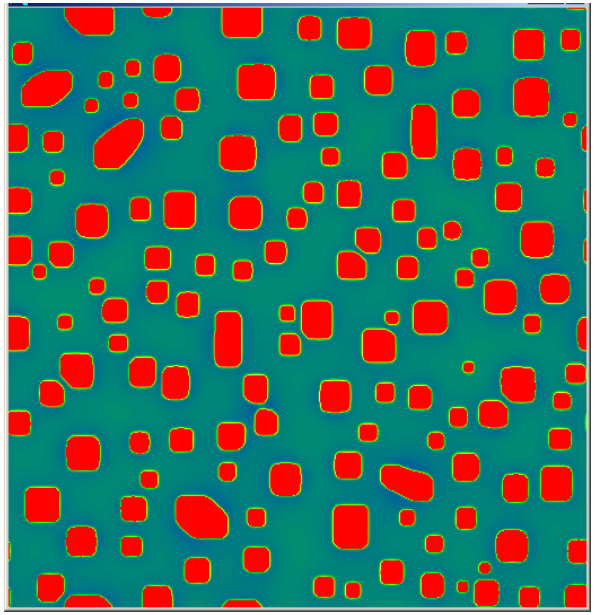

Equilibrium VF (450C) : 37.47%

Final Simulation AF : 30.35%

C = 0.143

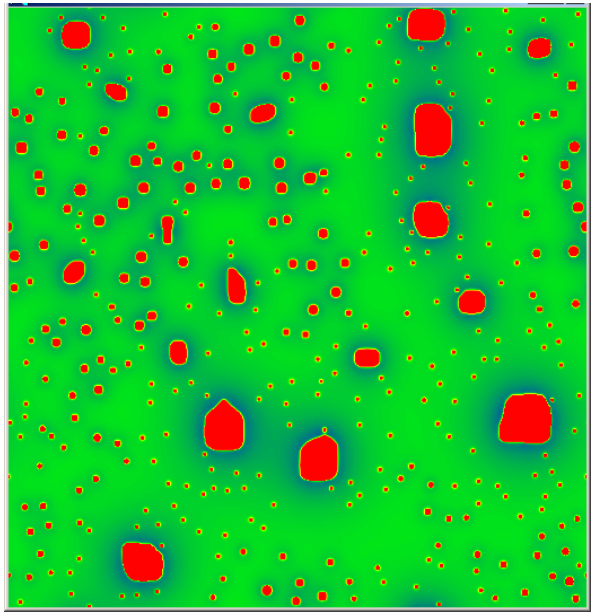

Equilibrium VF(450C) :30.83%

Final Simulation AF : 10.91%

γ′ rafting during creep

2 Slip Systems:(111)[10$\bar{1}$];(111)[01$\bar{1}$], positive Misfit, [001] Compression (>931MPa)

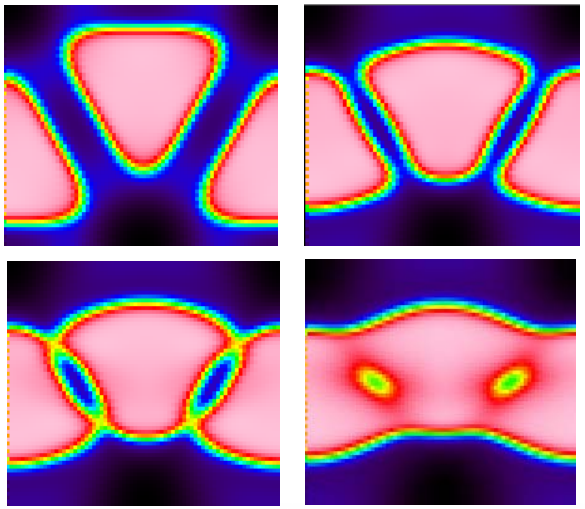

Time evolution - (111) cross-section

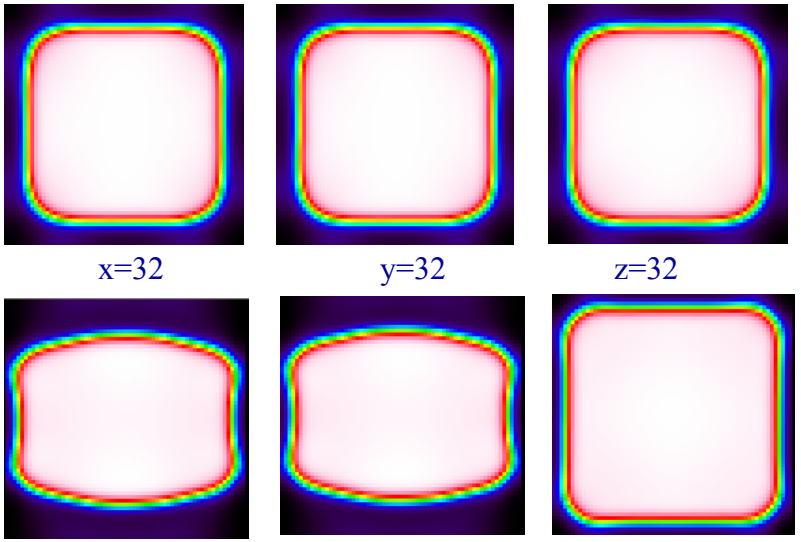

{100} cross-sections